NASA TECHNICAL MEMORANDUM

NASA TM X-2862

NASA TM X-2862

INFLUENCE OF ORBITAL-MANEUVERING-SYSTEM FAIRINGS AND RUDDER FLARE ON THE TRANSONIC AERODYNAMIC CHARACTERISTICS OF A SPACE SHUTTLE ORBITER

James C. Ellison

Langley Research Center
Hampton, Va. 23665

NATIONAL AERONAUTICS AND SPACE ADMINISTRATION • WASHINGTON, D. C. • FEBRUARY 1975

1. Report No.	2. Government Accession No.	3. Recipient's Catalog No.
NASA TM X-2862		

4. Title and Subtitle	5. Report Date
INFLUENCE OF ORBITAL-MANEUVERING-SYSTEM FAIRINGS AND RUDDER FLARE ON THE TRANSONIC AERODYNAMIC CHARACTERISTICS OF A SPACE SHUTTLE ORBITER	February 1975
	6. Performing Organization Code

7. Author(s)	8. Performing Organization Report No.
James C. Ellison	L-9580
	10. Work Unit No.
9. Performing Organization Name and Address	502-37-01-01
NASA Langley Research Center Hampton, Va. 23665	11. Contract or Grant No.
	13. Type of Report and Period Covered
12. Sponsoring Agency Name and Address	Technical Memorandum
National Aeronautics and Space Administration Washington, D.C. 20546	14. Sponsoring Agency Code

15. Supplementary Notes

16. Abstract

An investigation has been conducted in the Langley 8-foot transonic pressure tunnel to determine the influence of orbital-maneuvering-system fairings and a flared rudder on the aerodynamic characteristics of a space shuttle-orbiter configuration. Tests were made at Mach numbers from 0.4 to 1.2, at angles of attack from -1° to 24°, at angles of sideslip of 0° and 5°, and at a Reynolds number, based on model length, of 4×10^{6}. The model with the orbital-maneuvering-system fairings had a maximum untrimmed lift-drag ratio from 7.4 to 3.4 at Mach numbers from 0.4 to 1.2 and a maximum trimmed lift-drag ratio of about 3.55 at Mach 0.8 with the rudder flared 30°. The directional stability was increased at Mach 0.8 and 1.2 by addition of the orbital-maneuvering-system fairings and at Mach 1.2 by flaring the rudder.

17. Key Words (Suggested by Author(s))	18. Distribution Statement
Shuttle orbiter Transonic aerodynamics	Unclassified – Unlimited STAR Category 01

19. Security Classif. (of this report)	20. Security Classif. (of this page)	21. No. of Pages	22. Price*
Unclassified	Unclassified	36	$3.75

*For sale by the National Technical Information Service, Springfield, Virginia 22151

INFLUENCE OF ORBITAL-MANEUVERING-SYSTEM FAIRINGS AND RUDDER FLARE ON THE TRANSONIC AERODYNAMIC CHARACTERISTICS OF A SPACE SHUTTLE ORBITER

By James C. Ellison
Langley Research Center

SUMMARY

Transonic wind-tunnel tests have been conducted to determine the static longitudinal and lateral-directional aerodynamic characteristics of a space shuttle orbiter. Data were obtained at angles of attack from about -1° to 24°, at angles of sideslip of 0° and 5°, and at a Reynolds number, based on model length, of approximately 4.0×10^6. Mach numbers ranged from 0.4 to 1.2 with primary runs at Mach numbers of 0.8 and 1.2. The effects of orbital-maneuvering-system fairings, elevon deflection, and rudder flare on the aerodynamic characteristics were investigated.

The model with the orbital-maneuvering-system fairings had a maximum untrimmed lift-drag ratio from 7.4 to 3.4 at Mach numbers from 0.4 to 1.2 and a maximum trimmed lift-drag ratio of about 3.55 at Mach 0.8 with the rudder flared 30°.

Addition of the orbital-maneuvering-system fairings increased the directional stability of the model at Mach 0.8 and 1.2. Increasing the rudder flare also increased the directional stability at Mach 1.2. The directional stability parameter $C_{n_{\beta,dyn}}$ was positive throughout the test angle-of-attack range at Mach 0.8 and 1.2. However, at Mach 0.8 the value was markedly reduced at high angles of attack, where there was a region of negative effective dihedral.

INTRODUCTION

NASA and the aerospace industry are currently developing the space shuttle system for transporting large payloads to and from near-Earth orbit and for insertion of payloads for missions beyond Earth orbit. Early studies of this system focused on a fully reusable, two-stage system in which the orbiter vehicle is vertically launched and is capable of aircraft-type horizontal landing following reentry. This paper presents the results of an investigation of the transonic aerodynamic characteristics of the orbiter concept reported in reference 1 (which is a modification of the concept reported in ref. 2), designed for use in a fully reusable, two-stage shuttle system.

The investigation examined the effects of Mach number, component buildup (orbital-maneuver-system fairings and vertical tail), and flared rudder on the static longitudinal and lateral-directional aerodynamic characteristics. Also, effects of elevon deflection on longitudinal stability and of rudder flare on directional stability were investigated. Data were obtained in the Langley 8-foot transonic pressure tunnel at Mach numbers from 0.4 to 1.2, at angles of attack from -1° to 24°, at sideslip angles of 0° and 5°, and at a Reynolds number, based on model length, of 4.0×10^6.

SYMBOLS

The static longitudinal aerodynamic characteristics are presented in the stability-axis system, and the lateral-directional aerodynamic characteristics are presented in the body-axis system. The moment reference point corresponds to a center of gravity located at 67 percent of the body length and 41.4 percent of the maximum body height.

b reference span, 22.936 cm

C_D drag coefficient, $\frac{\text{Drag}}{qS}$

$C_{D,b}$ base-drag coefficient, $\frac{\text{Base drag}}{qS}$

C_L lift coefficient, $\frac{\text{Lift}}{qS}$

C_l rolling-moment coefficient, $\frac{\text{Rolling moment}}{qSb}$

C_{l_β} lateral-stability parameter, $\frac{\Delta C_l}{\Delta \beta}$, at $\beta = 0^{\circ}$ and $\beta = 5^{\circ}$

C_m pitching-moment coefficient, $\frac{\text{Pitching moment}}{qS\bar{c}}$

C_n yawing-moment coefficient, $\frac{\text{Yawing moment}}{qSb}$

C_{n_β} directional-stability parameter, $\frac{\Delta C_n}{\Delta \beta}$, at $\beta = 0^{\circ}$ and $\beta = 5^{\circ}$

$$C_{n_{\beta,dyn}} = C_{n_\beta} \cos \alpha - \frac{I_Z}{I_X} C_{l_\beta} \sin \alpha$$

C_Y side-force coefficient, $\frac{\text{Side force}}{qS}$

C_{Y_β} side-force parameter, $\frac{\Delta C_Y}{\Delta \beta}$, at $\beta = 0^o$ and $\beta = 5^o$

$\bar{c}$ mean aerodynamic chord, 13.142 cm

I_X moment of inertia about longitudinal body axis

I_Z moment of inertia about vertical body axis

L/D lift-drag ratio

M Mach number

q dynamic pressure, Pa

S reference area, 252.325 cm^2

α angle of attack, deg

α_{trim} angle of attack for $C_m = 0$, deg

β angle of sideslip, deg

δ_e elevon deflection angle, positive with trailing edge down, deg

δ_{flare} rudder flare angle, deg (see fig. 2)

Configuration designations and abbreviations:

BL buttock line, cm

B5 basic body

B9 basic body with OMS

FS fuselage station, cm

OMS orbital maneuvering system

V vertical tail

W wing

WL water line, cm

DESCRIPTION OF MODEL

A three-view sketch and cross-sectional views of the basic 0.00683-scale model are presented in figure 1. The wing, having an aspect ratio of 2.08 based on the wing theoretical planform area, had an NACA 0010-64 airfoil at the wing-body juncture and an NACA 0012-64 airfoil at 81.7 percent of the semispan. The elevons had provisions for deflection angles of 0°, -15°, and -30°. Details of the vertical tail and rudder are presented in figure 2. Interchangeable rudders with flare angles of 0°, 15°, and 30° could be mounted on the vertical tail. Details and location of the OMS fairings are shown in figure 3.

TESTS AND PROCEDURES

The tests were conducted in the Langley 8-foot transonic pressure tunnel (ref. 3) at Mach numbers from 0.4 to 1.2 and at a Reynolds number, based on model length, of approximately 4.0×10^{6}. Transition was fixed by placing 0.159-cm-wide strips of No. 120 carborundum grit at locations 3.81 cm from the nose and 1.27 cm from the leading edges of the wing and vertical tail. Forces and moments were measured with a sting-supported, six-component, strain-gage balance. Base pressure measurements were obtained at two locations. The angle of attack was varied from -1° to 24° at angles of sideslip of 0° and 5°.

Angles of attack and sideslip have been corrected for the effects of sting and balance deflections due to aerodynamic loads and for tunnel flow angularity. The drag coefficients represent gross drag in that no correction was made for base drag or grit drag (assumed negligible). However, base-drag coefficients, calculated from the average of the measured base pressures, are presented.

RESULTS AND DISCUSSION

Flight Attitudes and Control Settings

In the transonic speed regime the orbiter trim angle of attack was assumed to be 10°, as shown by the nominal entry angle-of-attack schedule in figure 4.

The flared rudder was designed to provide increased directional stability at high Mach numbers. In the upper speed range of this investigation (M = 0.8 to 1.2), $\delta_{flare} = 30^{\circ}$; in the subsonic regime, $\delta_{flare} = 0^{\circ}$ to reduce base drag.

Longitudinal Aerodynamic Characteristics

Effect of Mach number.- The effect of Mach number on the longitudinal aerodynamic characteristics for the complete configuration (vertical tail and OMS fairings mounted) is shown in figure 5. For $\alpha < 12^{\circ}$ there were only small changes in lift-curve slope with increasing Mach number. However, above $\alpha = 12^{\circ}$ the lift-curve slopes varied to such an extent that for $\alpha = 24^{\circ}$ the values of C_L ranged from about 0.9 to 1.2. The maximum values of L/D varied from about 3.4 at M = 1.2 to 7.4 at M = 0.4. The configuration was stable at $\alpha < 16^{\circ}$, but at some angle of attack above 16° (depending on Mach number), the configuration became longitudinally unstable.

Effect of vertical tail and OMS fairings.- Data obtained at M = 0.8 and 1.2 are presented in figures 6 and 7, respectively, for the basic configuration with the vertical tail removed (B5W), the basic configuration (B5WV), and the basic configuration with the OMS fairings (B9WV). The addition of the vertical tail had little effect on the longitudinal characteristics except for a small decrease in the maximum of L/D at M = 0.8 and 1.2 and a positive pitching-moment increment at M = 1.2. Addition of the OMS fairing produced a positive increment in C_m of about 0.004 at M = 0.8 and 0.012 at M = 1.2 and a reduction in the maximum untrimmed L/D of about 1.0 at M = 0.8.

Effect of rudder flare.- The effects of rudder flare angle at M = 1.2 for the basic configuration are shown in figure 8. Increasing the rudder flare angle from 0° to 60° produced a nearly constant increment in C_L, C_D, and C_m over the angle-of-attack range, decreasing C_L while increasing C_D and C_m. The data indicate a substantial loss in L/D. In fact, at $\alpha = 10^{\circ}$, L/D is reduced from 3.5 to 2.9, and the maximum untrimmed L/D is reduced from 3.7 to 2.9 by flaring the rudder 60°. Longitudinal stability was essentially unaffected by rudder flare.

Effect of elevon deflection.- Through the Mach number range 0.8 to 1.2, the schedule for rudder flare called for $\delta_{flare} = 30^{\circ}$; therefore, the effect of elevon deflection was obtained on configurations with a rudder flare angle of 30°. The data for the B9WV configuration with $\delta_e = 0^{\circ}$, -15°, and -30° at M = 0.8 are presented in figure 9, and the data for the B5WV configuration with $\delta_e = 0^{\circ}$ and -30° at M = 1.2 are presented in figure 10. Data for the B5WV configuration (M = 1.2) indicate that at $\delta_e = -30^{\circ}$, trim occurs at about $\alpha = 9.5^{\circ}$, slightly below the scheduled angle of attack ($\alpha = 10^{\circ}$). However, the results presented in figure 9 indicate that with the OMS fairings, the configuration would trim at $\alpha \approx 10^{\circ}$ with slightly less negative elevon deflection.

The trim characteristics of the B9WV configuration at $M = 0.8$ are summarized in figure 11. The configuration was trimmable over the angle-of-attack range. At $\alpha = 10^{\circ}$ the configuration required $\delta_e = -9.2^{\circ}$ for trim and had a trimmed L/D of 3.4, which was only about 0.15 less than the maximum trimmed L/D.

Lateral-Directional Aerodynamic Characteristics

The lateral-directional parameters C_{l_β}, C_{n_β}, and C_{Y_β} (figs. 12 and 13) were calculated from the increments in C_l, C_n, and C_Y, respectively, at $\beta = 0^{\circ}$ and 5°. Therefore, they do not account for any nonlinearities which may exist in the intermediate sideslip range.

Effect of vertical tail and OMS fairings.- The lateral-directional parameters C_{l_β}, C_{n_β}, and C_{Y_β} are shown in figure 12 for the B5W, B5WV, and B9WV configurations at $M = 0.8$ and 1.2. At $M = 0.8$ (fig. 12(a)) the model without the vertical tail was directionally unstable and had large positive values of C_{l_β} (negative dihedral effect) above $\alpha = 5^{\circ}$. Addition of the vertical tail and the OMS fairings provided a positive increment in C_{n_β}, and the model was directionally stable over the test angle-of-attack range. The vertical tail and OMS also increased the effective dihedral of the model (negative increment in C_{l_β}). However, between $\alpha = 10^{\circ}$ and 20°, the values of C_{l_β} were positive. The angle of attack at which the loss in effective dihedral occurs appears to be a function of Mach number, since data from reference 2 for a comparable model indicated positive effective dihedral up to angles of attack of about 19°. The vertical tail and OMS provided positive effective dihedral $\left(-C_{l_\beta}\right)$ throughout the test angle-of-attack range at $M = 1.2$ also (fig. 12(b)) but were less effective in providing directional stability than at $M = 0.8$. With the vertical tail the model was directionally stable at $\alpha < 9.6^{\circ}$, and with the OMS the model was stable up to $\alpha = 19^{\circ}$.

Effect of rudder flare.- The lateral-directional characteristics of the B5WV configuration with $\delta_{flare} = 0^{\circ}$, 30°, and 60° at $M = 1.2$ are shown in figure 13. The effect of rudder flare was to extend the directional stability from $\alpha = 10^{\circ}$ to about $\alpha = 19.6^{\circ}$ with 30° of flare and to the highest test angle of attack with 60° of flare. The effective dihedral increased by about 0.001 for $\alpha < 20^{\circ}$ when the rudder flare angle was increased from 0° to 60°.

Directional-stability criterion.- The dynamic directional-stability parameter $C_{n_{\beta,dyn}}$ (see ref. 4), which represents a criterion for directional stability, was computed by using data for zero elevon deflection from figure 12 and is presented in figure 14. Although it is recognized that deflection of the elevons for trim will affect the lateral-directional characteristics (see ref. 2), the longitudinal trim data at sideslip were not available, and therefore, the data are presented for the untrimmed case. Positive values

of the parameter $C_{n_{\beta,dyn}}$ are shown to exist throughout the angle-of-attack range for both $M = 0.8$ and 1.2. In general, this indicates that the possibility of directional divergence at the nominal angle of attack is small. At $M = 0.8$, however, $C_{n_{\beta,dyn}}$ decreases markedly and reaches a minimum value at angles of attack from 16° to 18°. This reduction in $C_{n_{\beta,dyn}}$ is caused by the positive values of C_{l_β} (negative effective dihedral) shown in figure 12(a). In reference 4, it is pointed out that positive values of $C_{n_{\beta,dyn}}$ combined with negative effective dihedral can result in yaw divergence if the yaw due to aileron deflection is favorable (if C_n/C_l is positive for aileron deflection). In reference 5 this ratio is positive at $M = 0.8$ for angles of attack up to 17°.

SUMMARY OF RESULTS

Transonic wind-tunnel tests have been conducted to determine the static longitudinal and lateral-directional aerodynamic characteristics of a space shuttle orbiter and the effects of an orbital maneuvering system, elevon deflection, and rudder flare on these characteristics. The results of the investigation are summarized as follows:

1. The model with the orbital-maneuvering-system fairings had a maximum untrimmed lift-drag ratio from 7.4 to 3.4 at Mach numbers from 0.4 to 1.2 and a maximum trimmed lift-drag ratio of about 3.55 at Mach 0.8 with the rudder flared 30°.

2. Addition of the orbital-maneuvering-system fairings increased the directional stability of the model at Mach 0.8 and 1.2 and increased the angle-of-attack range for directional stability at Mach 1.2. Increasing the rudder flare also produced sizable increases in directional stability at Mach 1.2.

3. The dynamic directional-stability parameter $C_{n_{\beta,dyn}}$ was positive throughout the test angle-of-attack range at Mach 0.8 and 1.2. However, at Mach 0.8 the value was markedly reduced at high angles of attack, where there was a region of negative effective dihedral.

Langley Research Center,
National Aeronautics and Space Administration,
Hampton, Va., December 17, 1974.

REFERENCES

1. Putnam, Lawrence E.: Aerodynamic Characteristics of an Ogee-Wing Space-Shuttle Orbiter Concept at a Mach Number of 2.01. NASA TM X-2473, 1972.

2. Ellison, James C.: Subsonic Aerodynamic Characteristics of a Space Shuttle Orbiter. NASA TM X-2786, 1973.

3. Schaefer, William T., Jr.: Characteristics of Major Active Wind Tunnels at the Langley Research Center. NASA TM X-1130, 1965.

4. Moul, Martin T.; and Paulson, John W.: Dynamic Lateral Behavior of High-Performance Aircraft. NACA RM L58E16, 1958.

5. Intrieri, Peter F.; and White, L. S.: Aerodynamic Characteristics of McDonnell-Douglas Delta Wing Orbiter at Mach Numbers From 0.6 to 2.0. NASA TM X-62042, 1971.

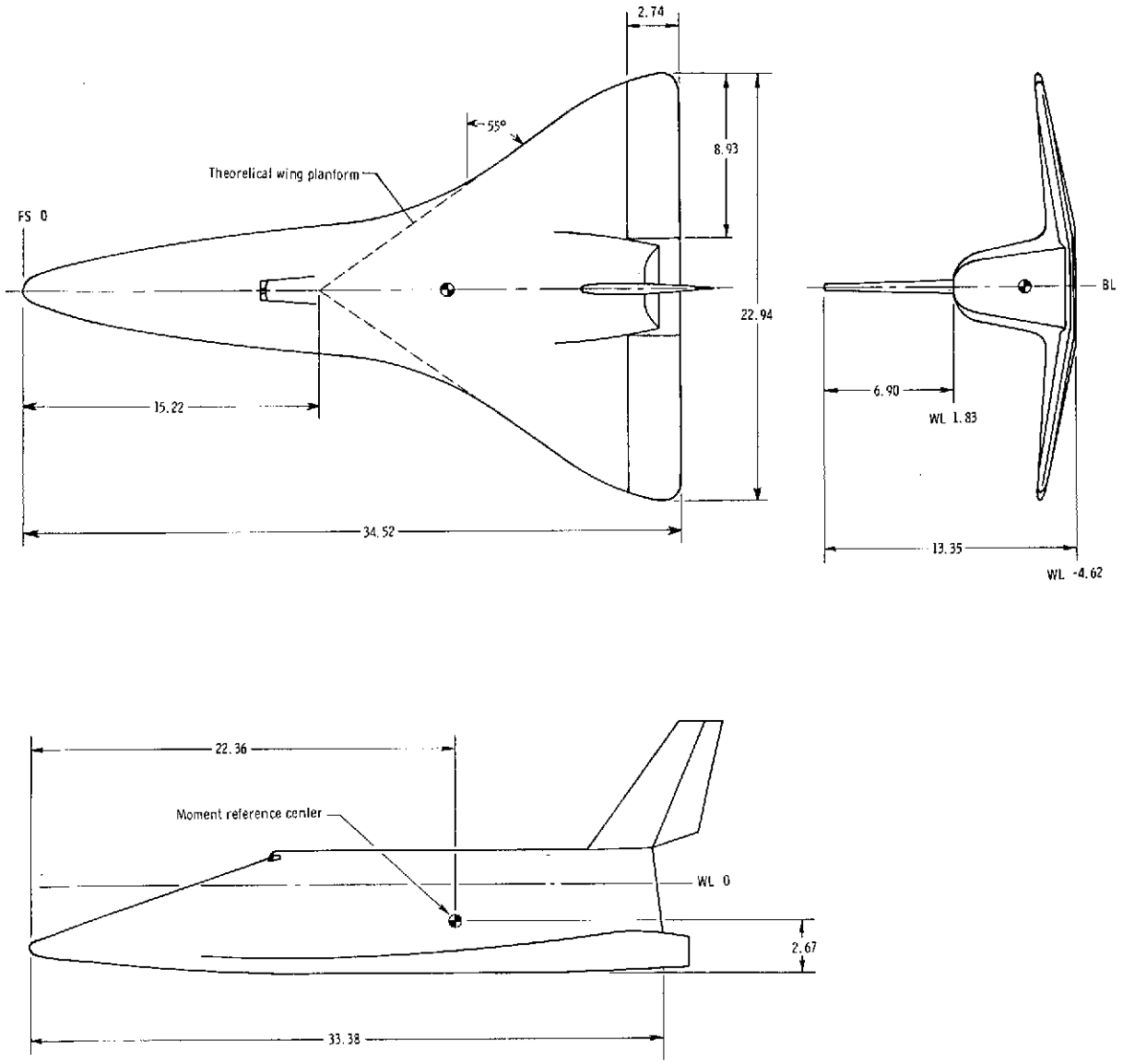

(a) Three-view drawing of basic model.

Figure 1.- Details of basic configuration model (B5WV).
All linear dimensions are in centimeters.

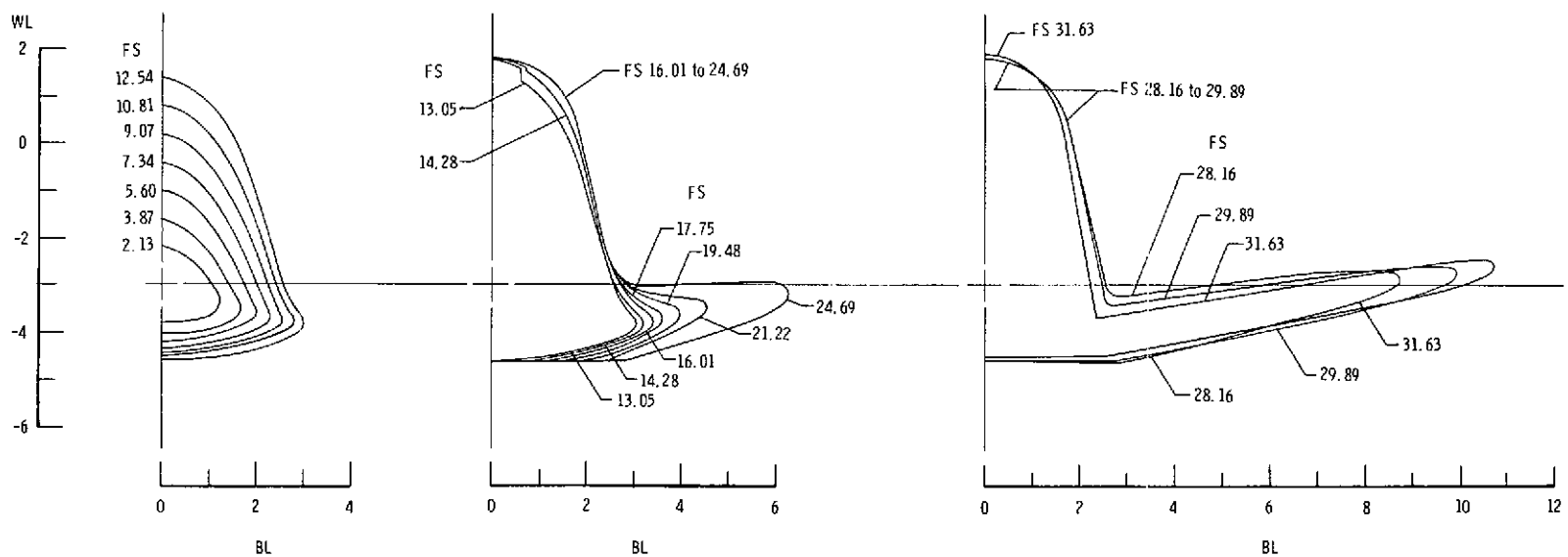

(b) Cross sections of the model.

Figure 1.- Concluded.

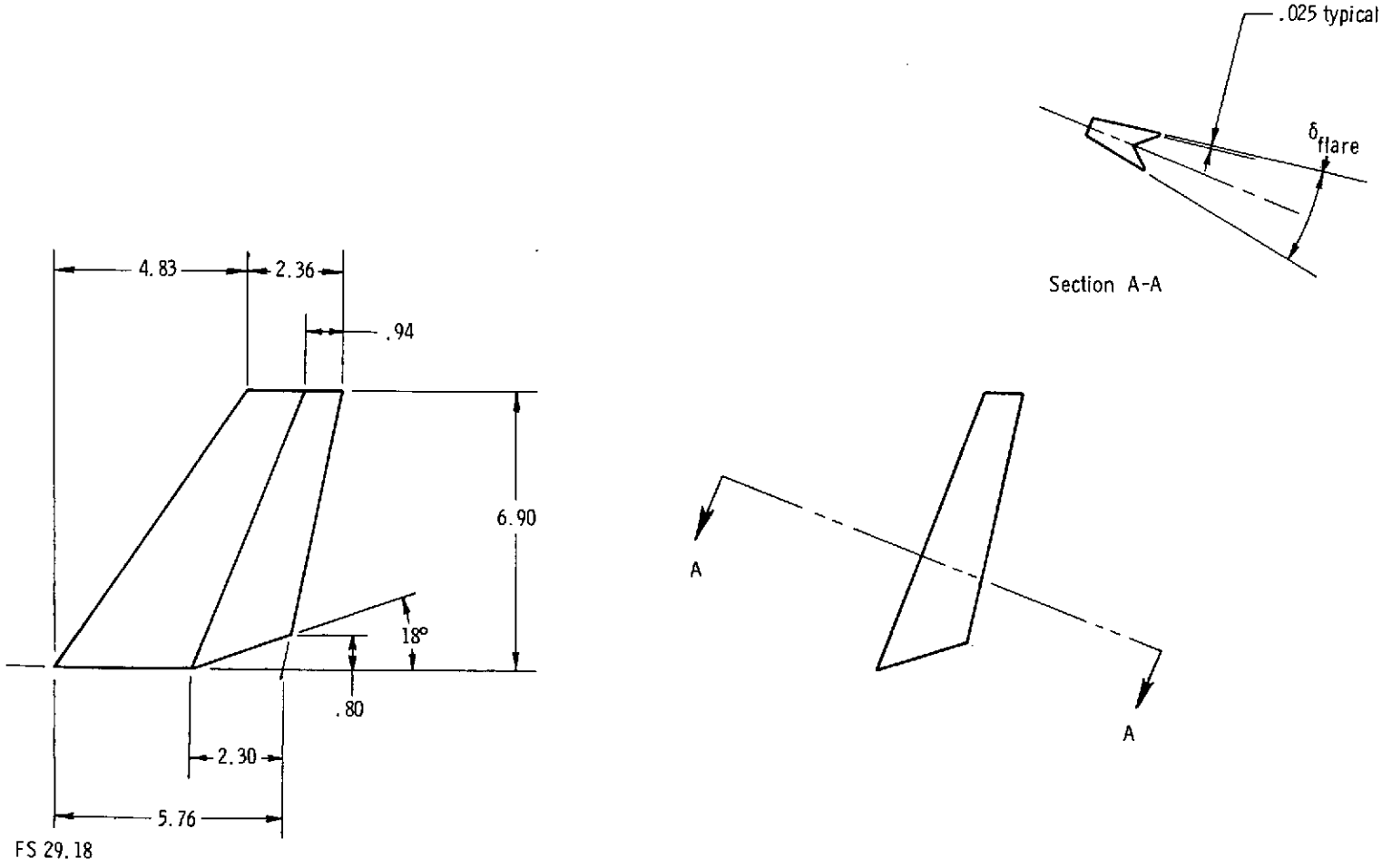

Figure 2.- Details of vertical tail and flared rudder. All linear dimensions are in centimeters.

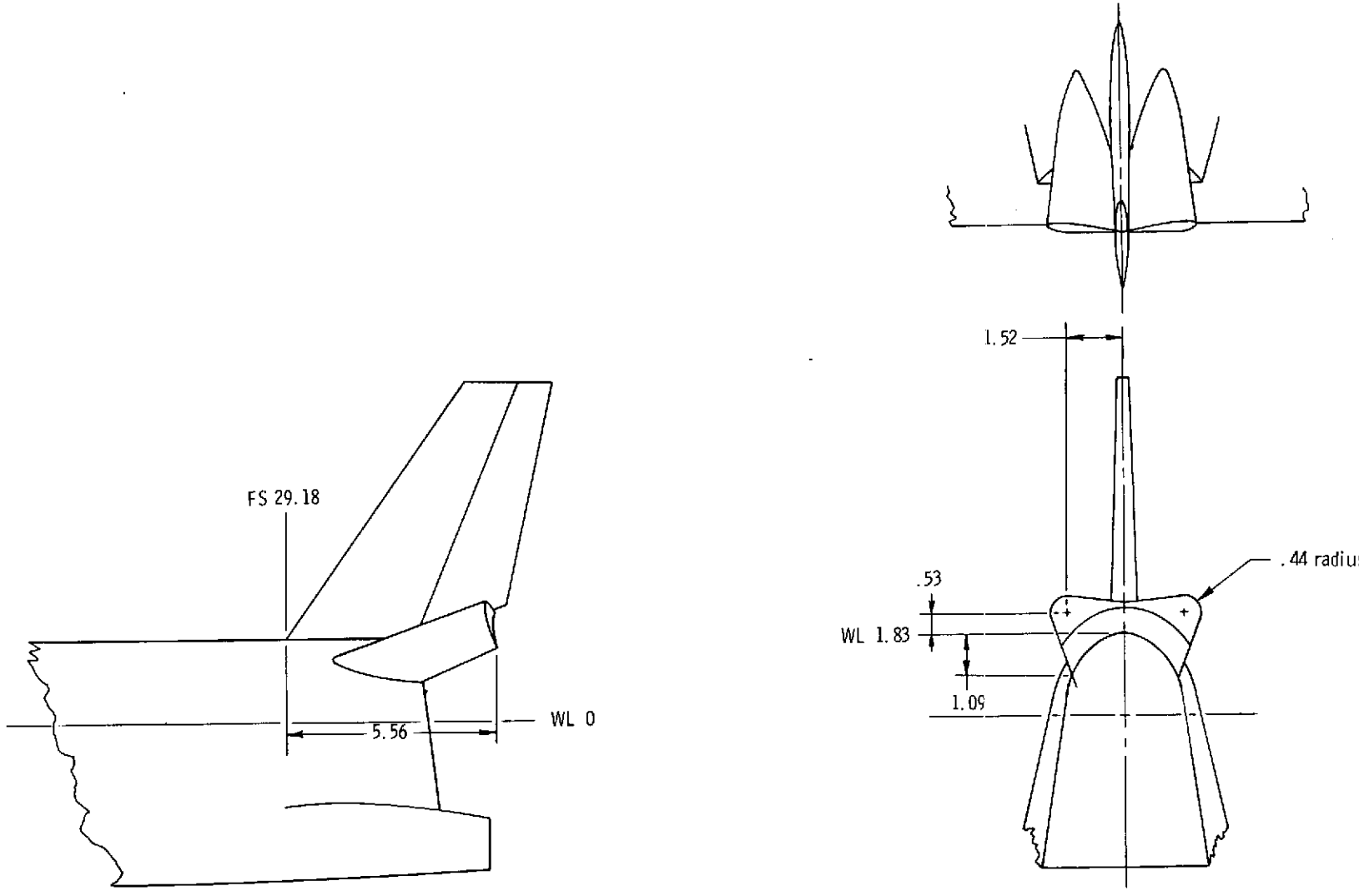

Figure 3.- Details of OMS fairings (configuration B9). All linear dimensions are in centimeters.

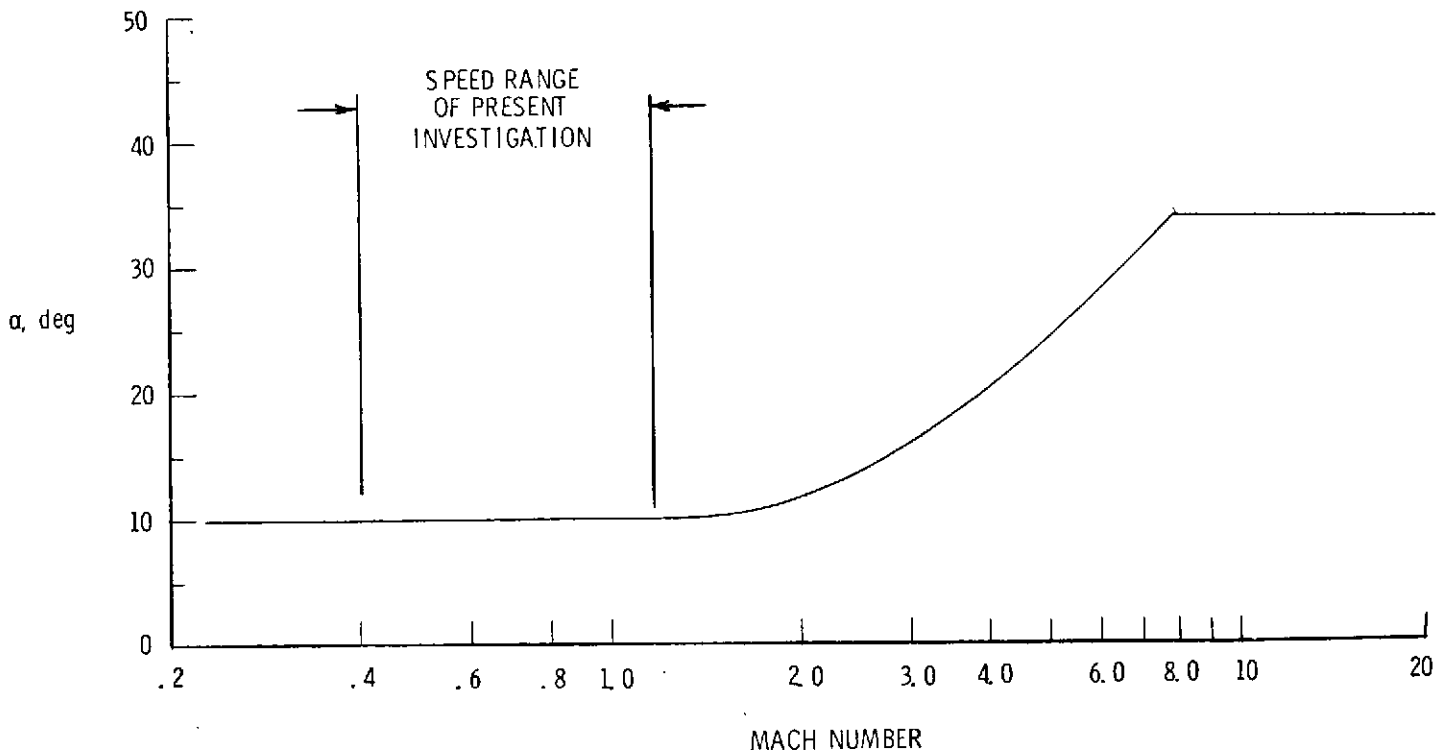

Figure 4.- Nominal entry angle-of-attack schedule.

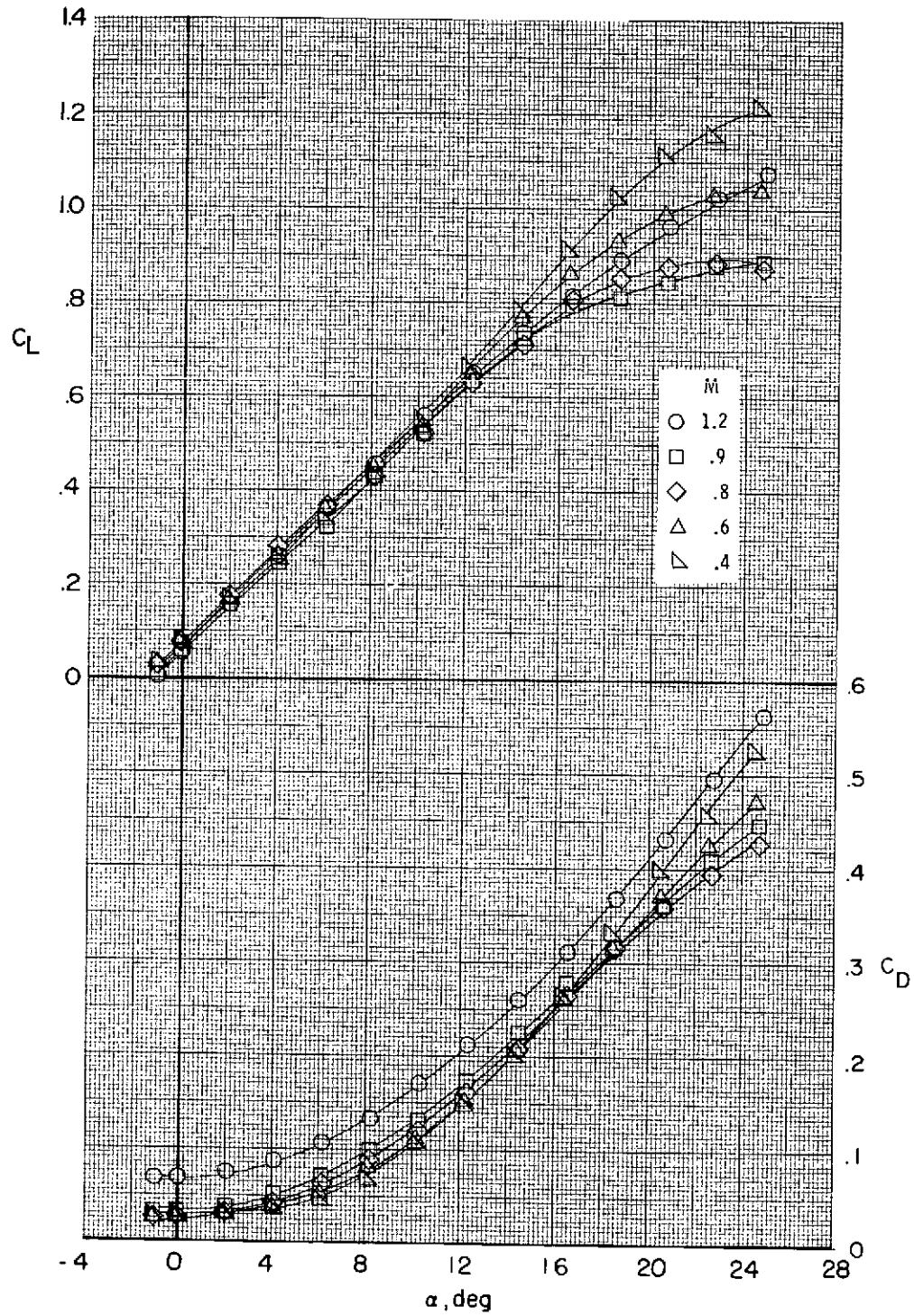

Figure 5.- Effect of Mach number on longitudinal aerodynamic characteristics for B9WV. $\delta_e = 0^o$.

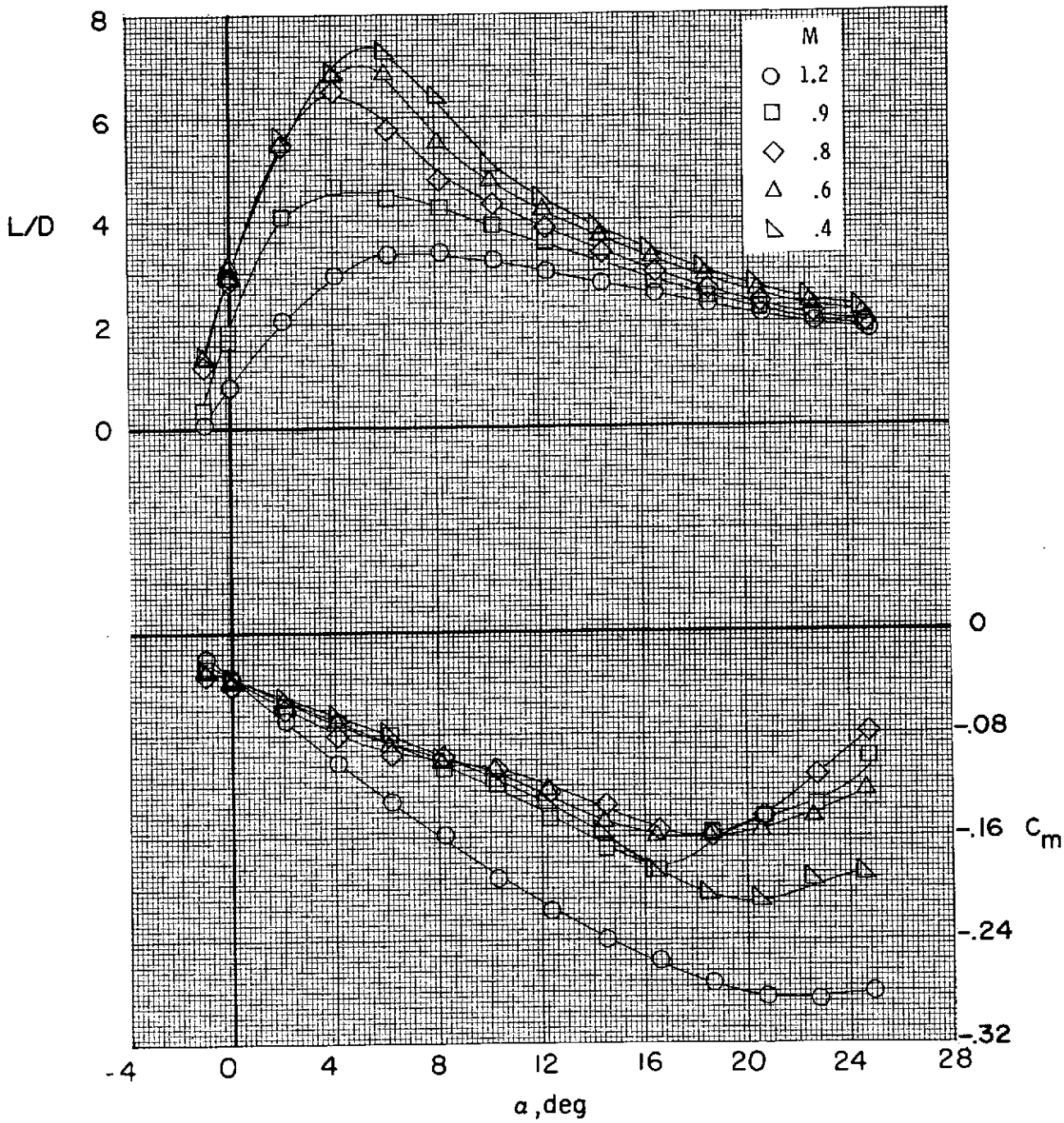

Figure 5.- Continued.

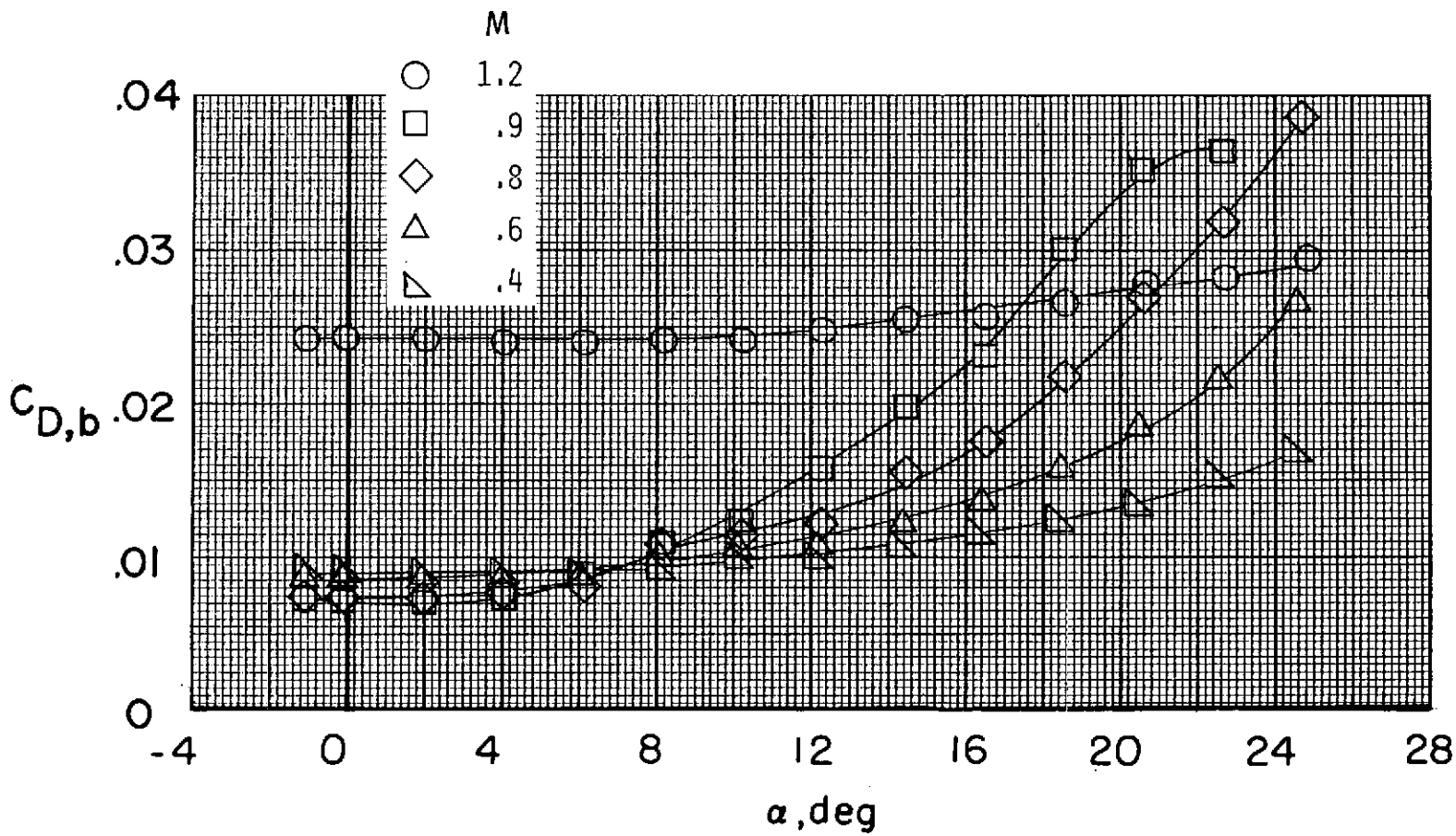

Figure 5.- Concluded.

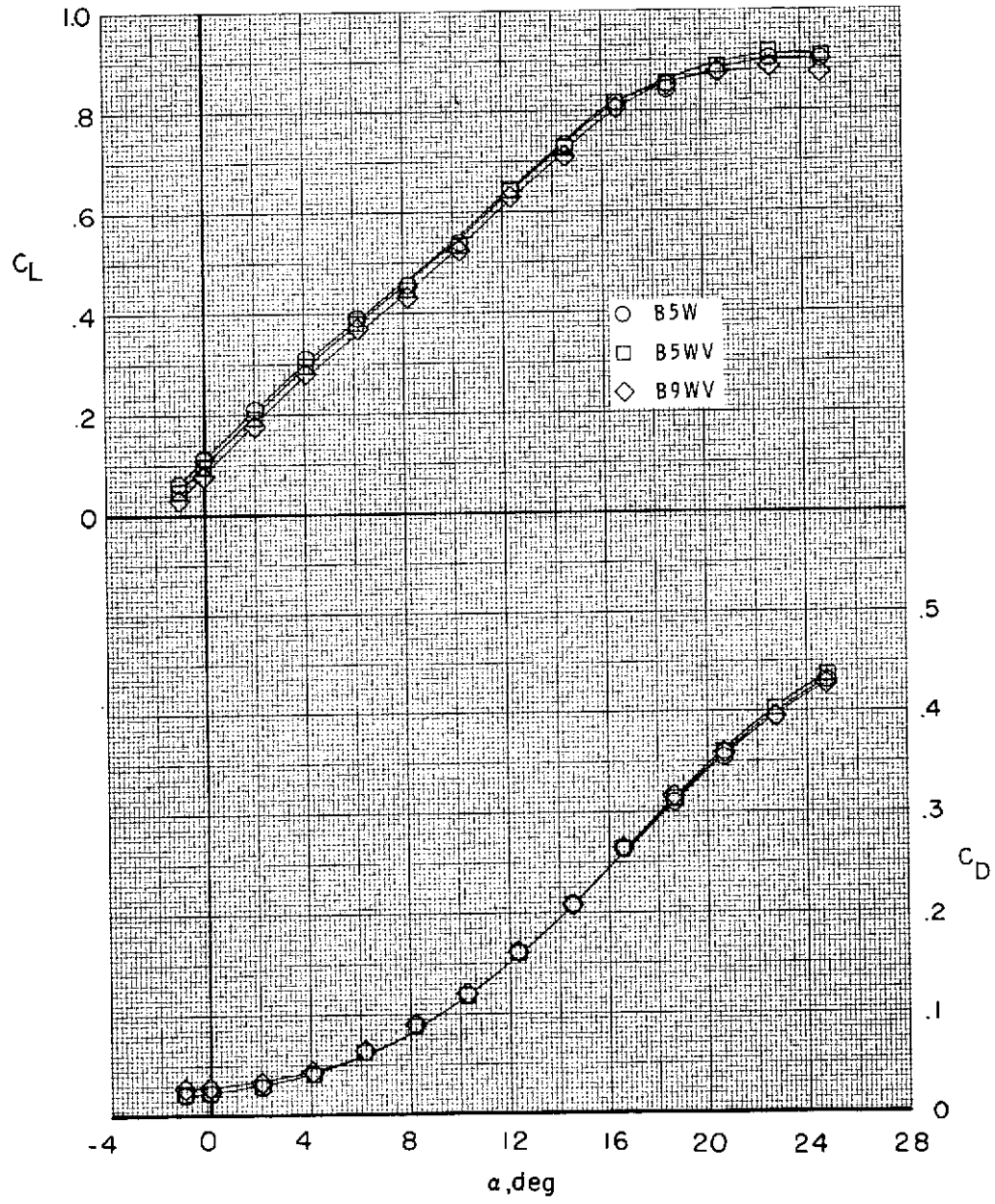

Figure 6.- Effect of component buildup on longitudinal aerodynamic characteristics at $M = 0.8$. $\delta_e = 0^o$.

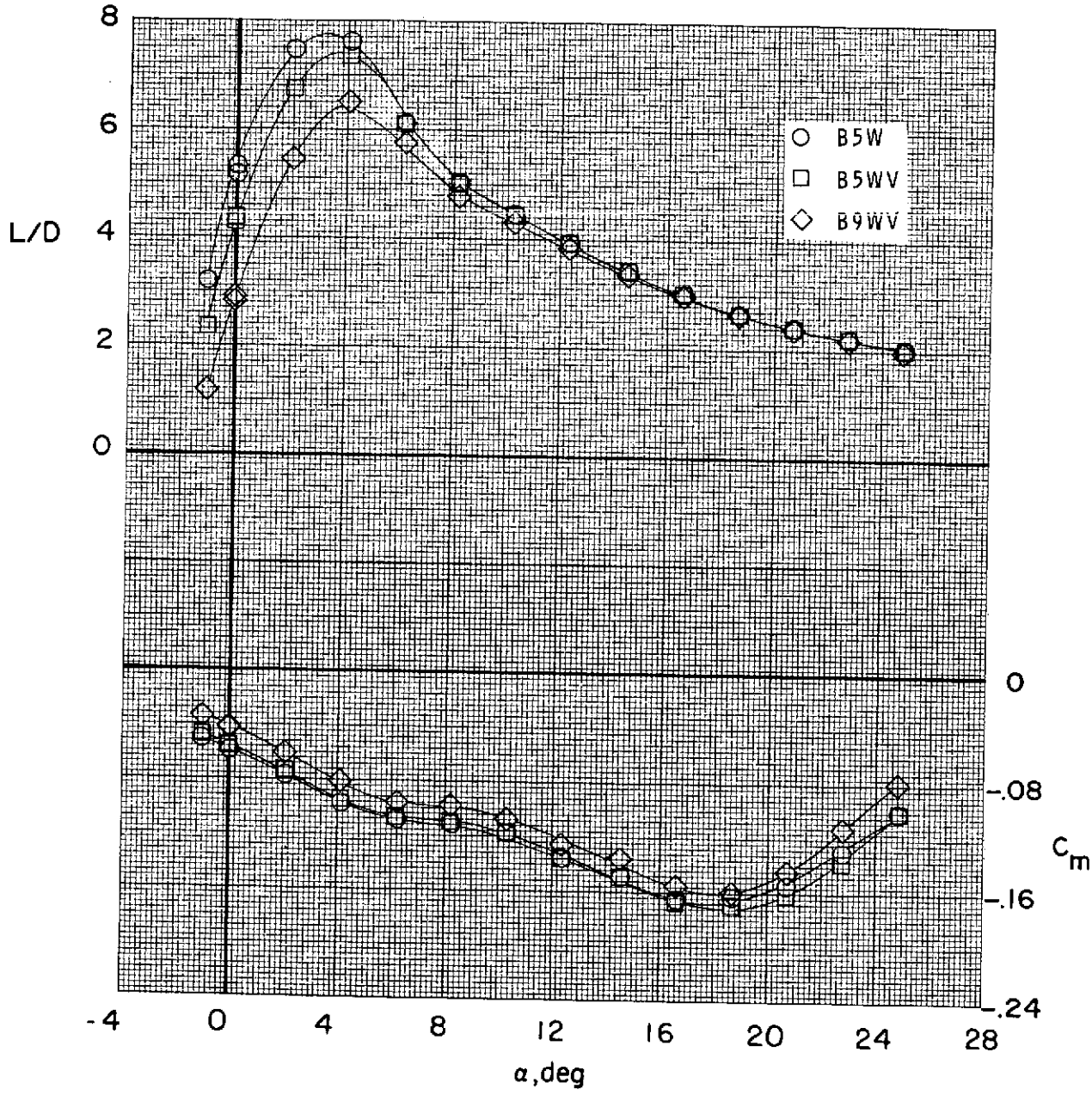

Figure 6.- Continued.

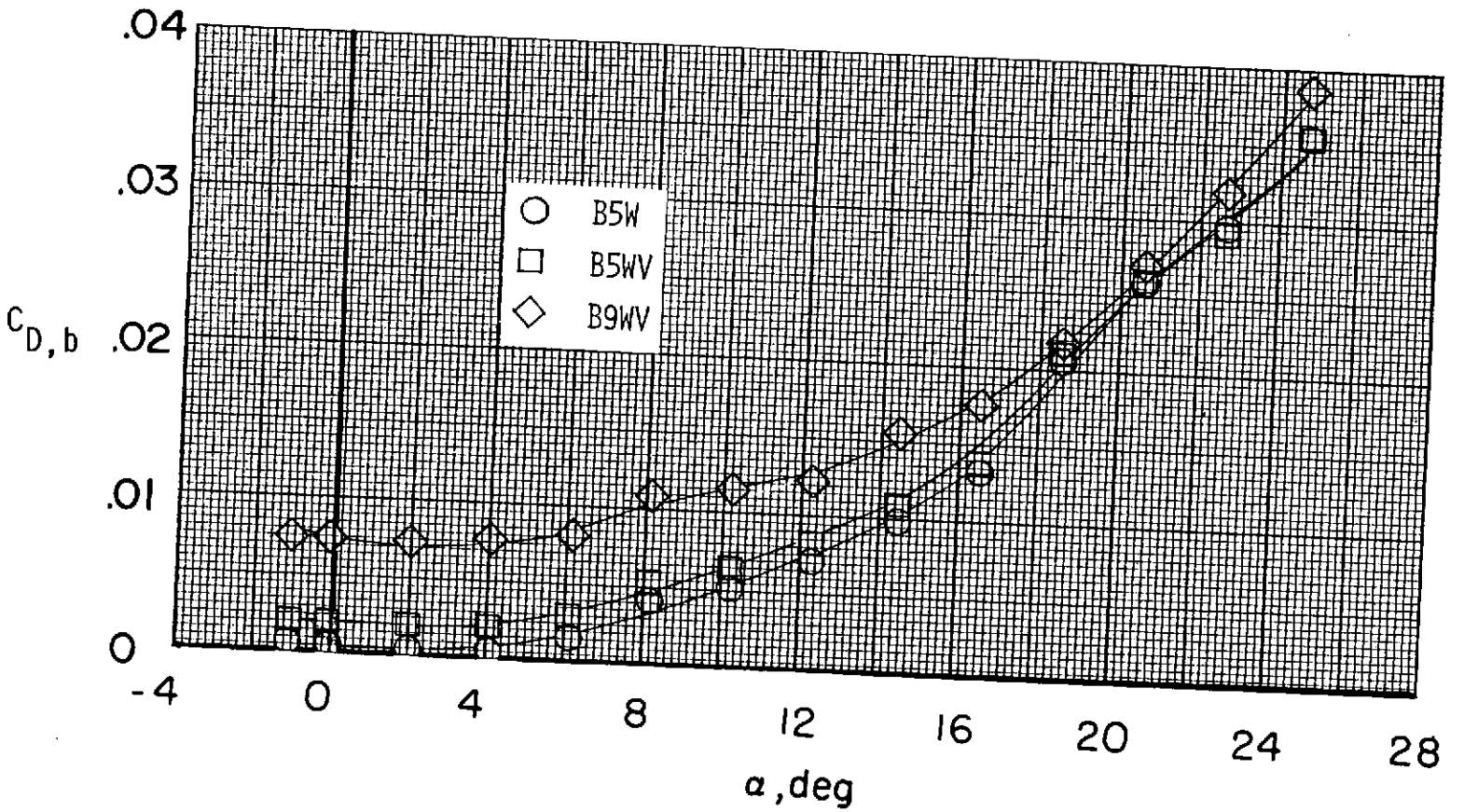

Figure 6.- Concluded.

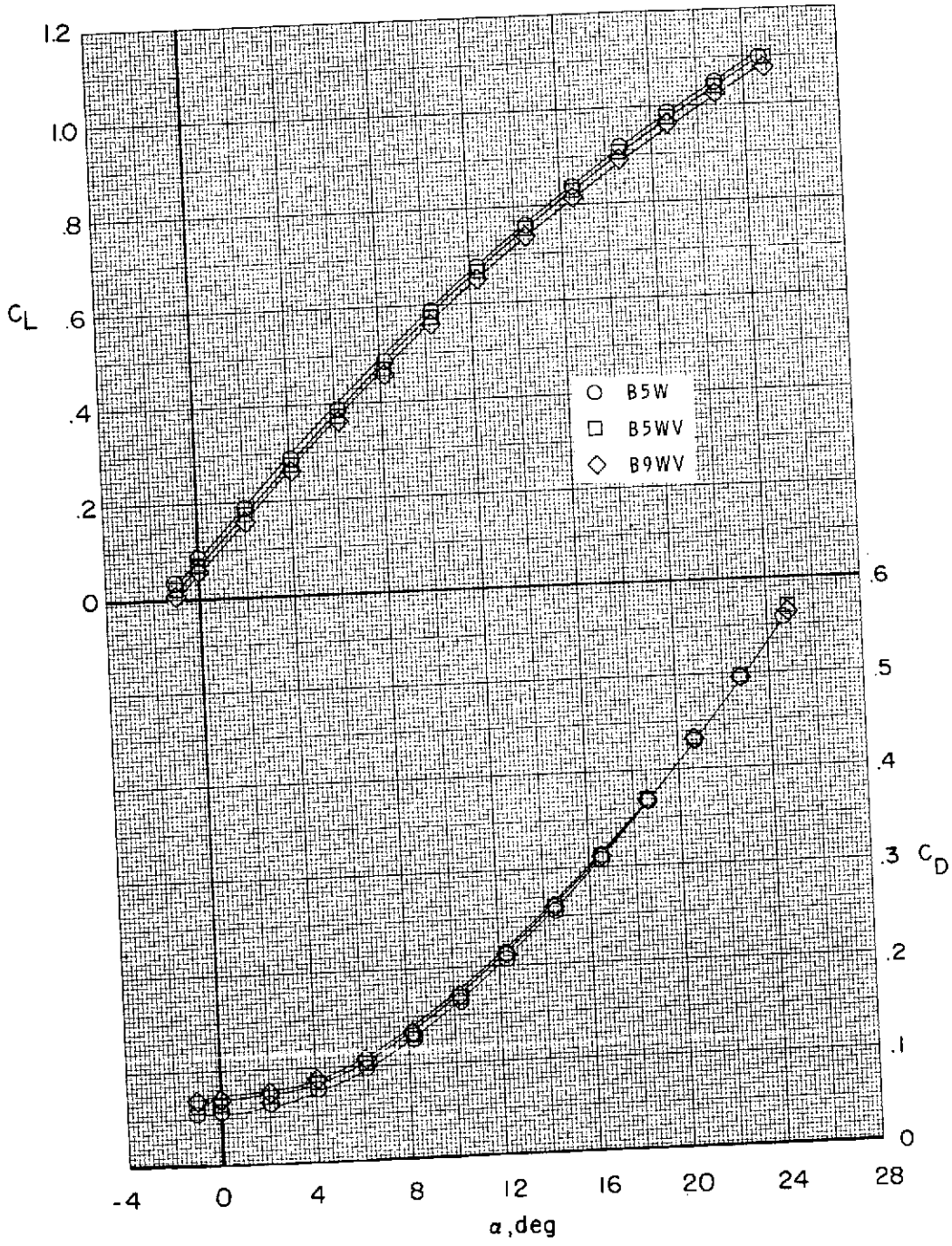

Figure 7.- Effect of component buildup on longitudinal aerodynamic characteristics at $M = 1.2$. $\delta_e = 0^o$.

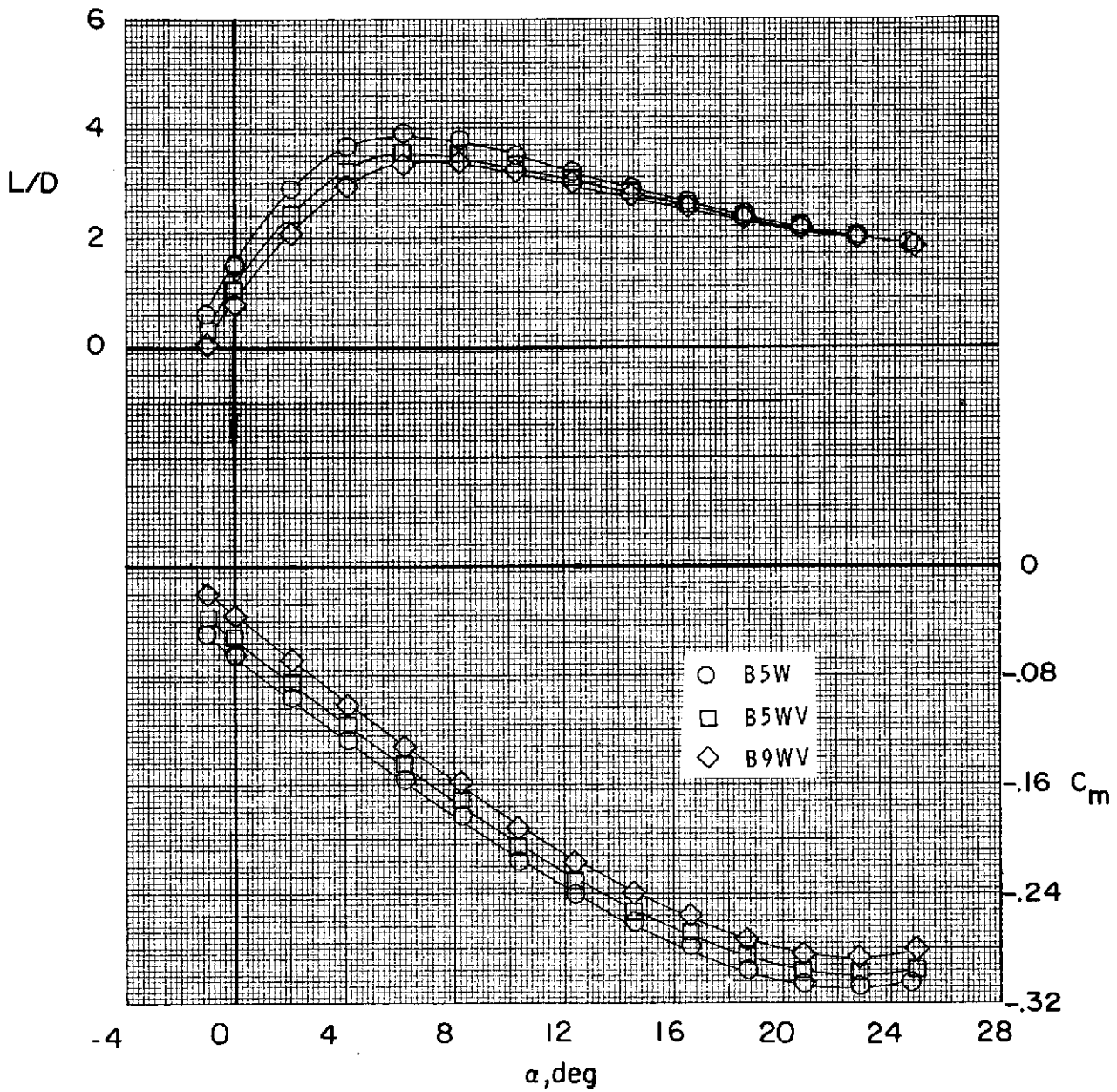

Figure 7.- Continued.

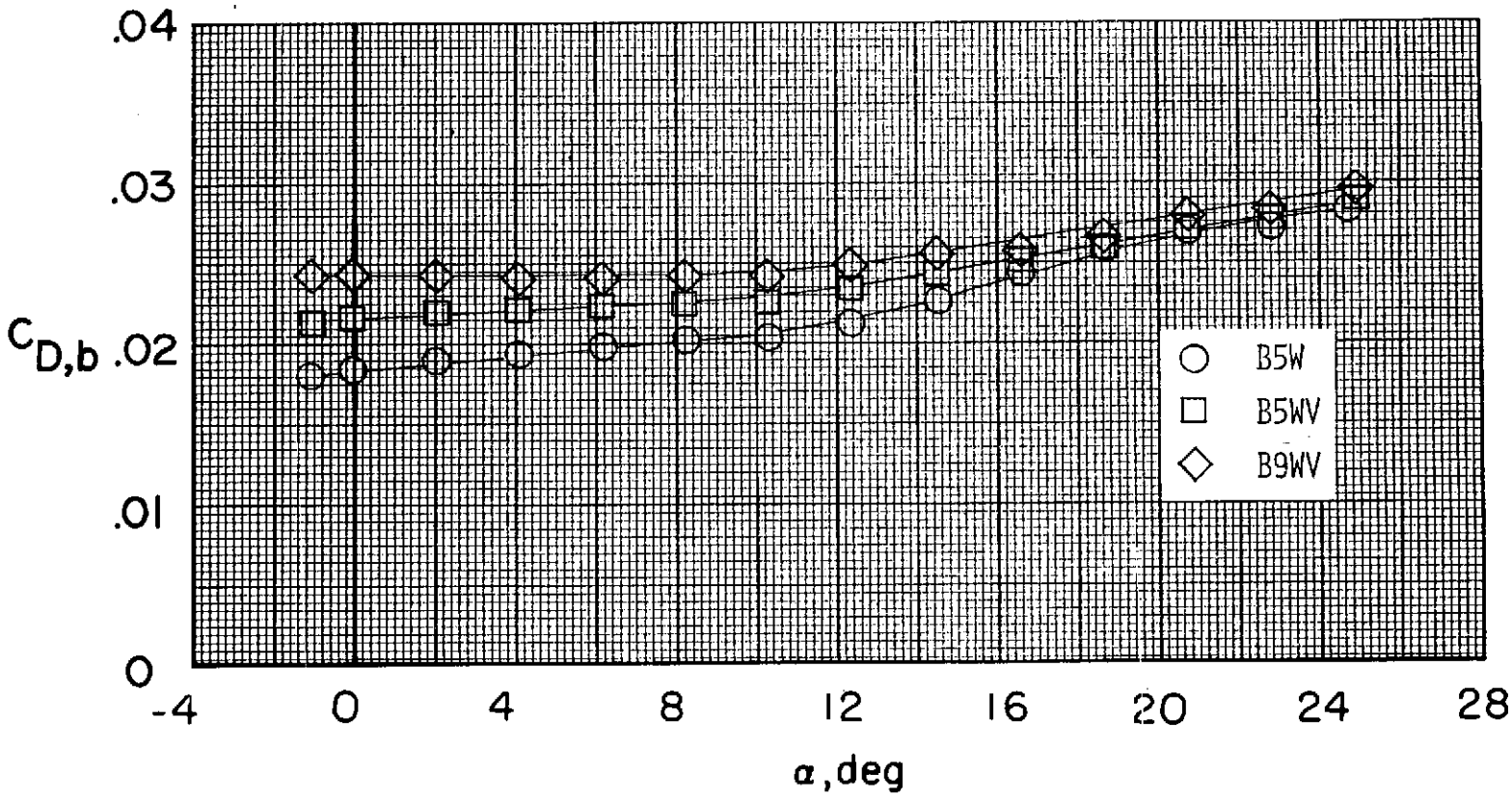

Figure 7.- Concluded.

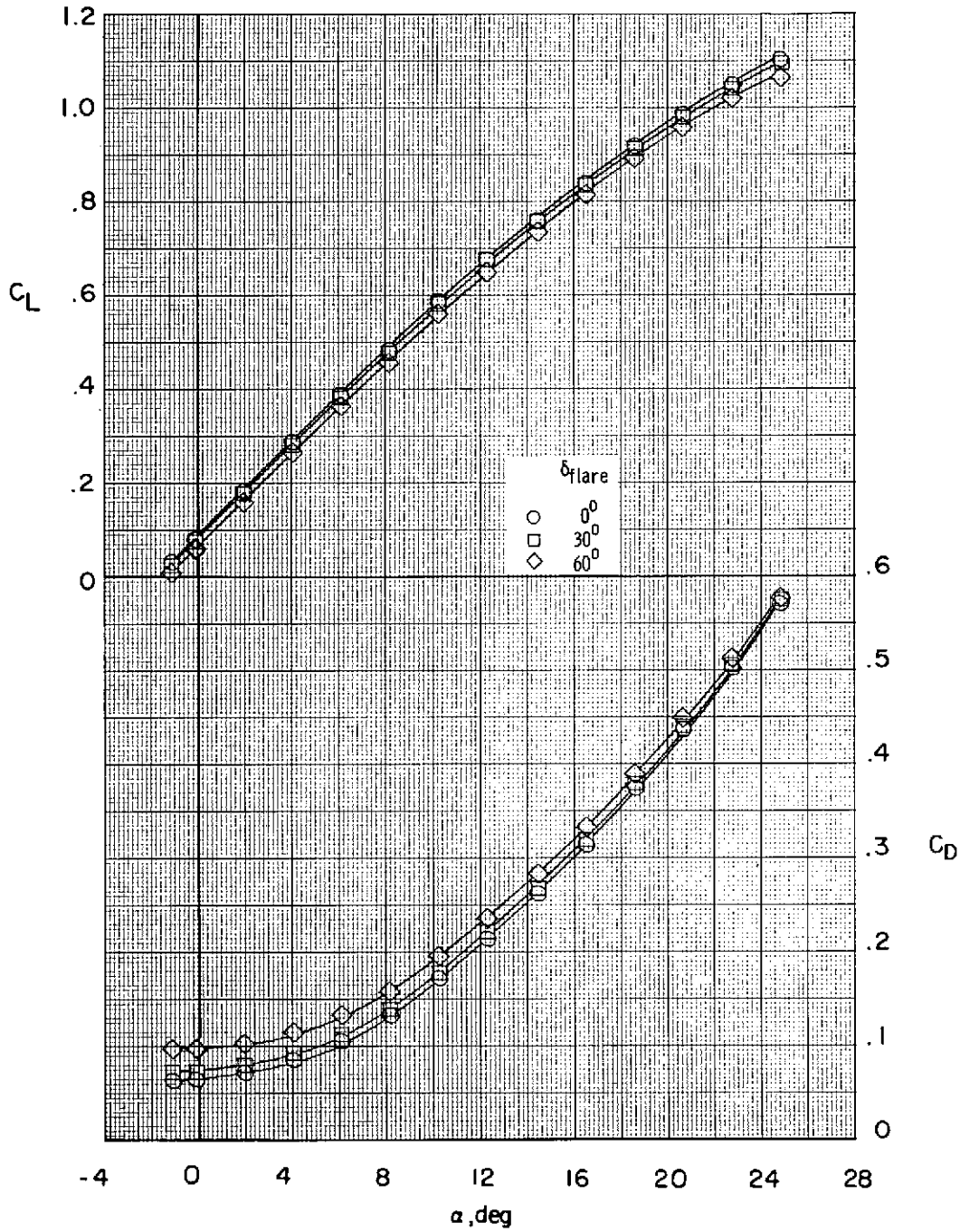

Figure 8.- Effect of rudder flare on longitudinal aerodynamic characteristics for B5WV. M = 1.2; $\delta_e = 0^o$.

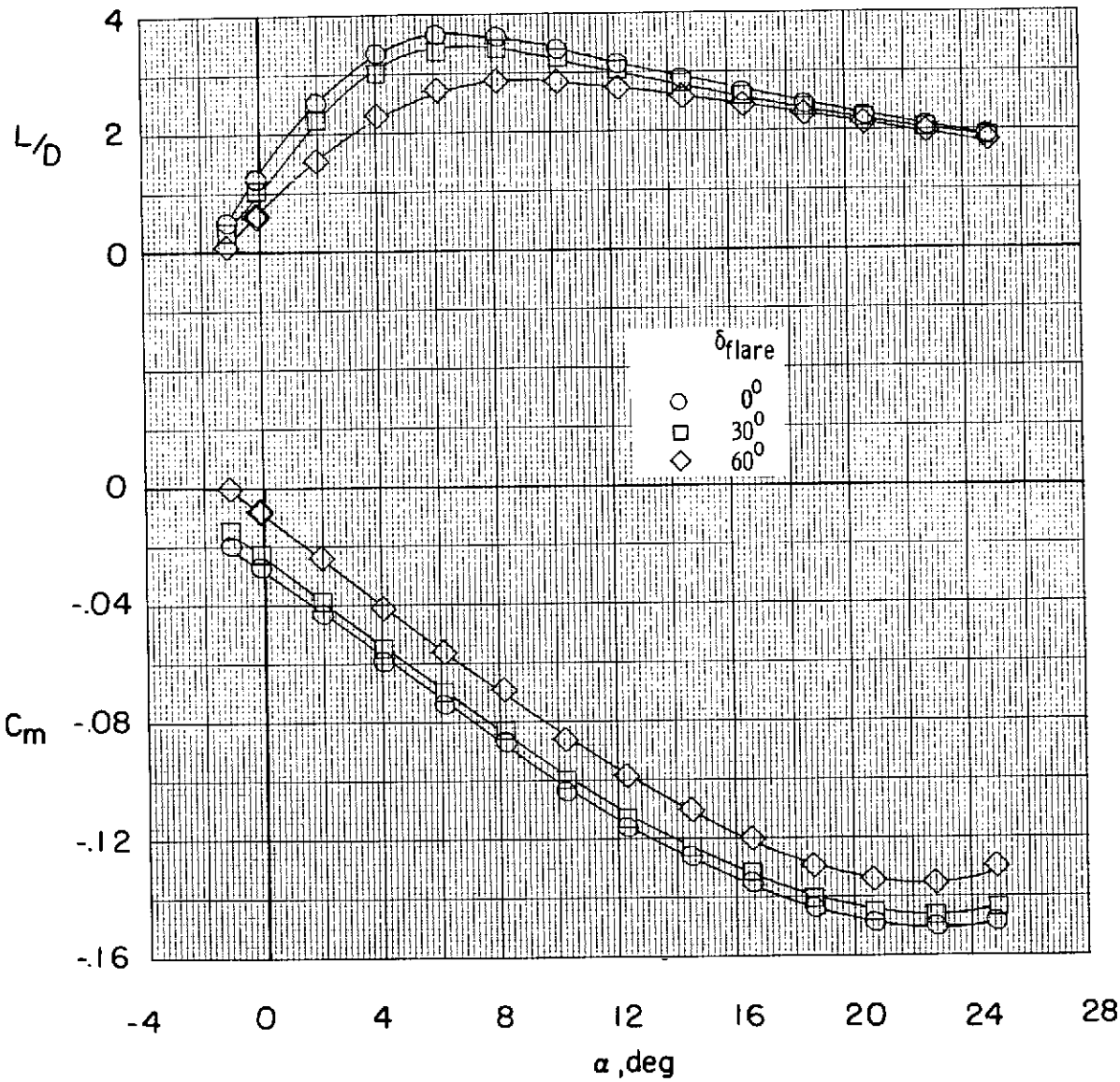

Figure 8.- Continued.

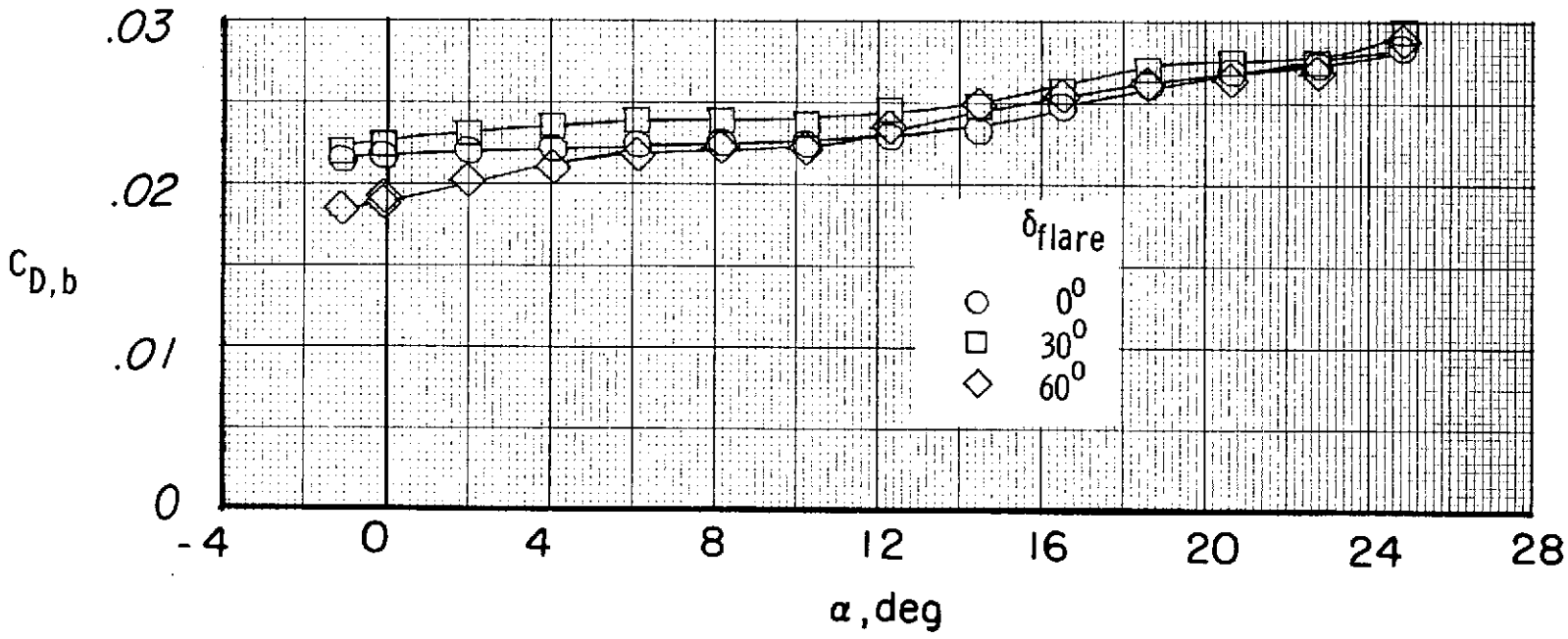

Figure 8.- Concluded.

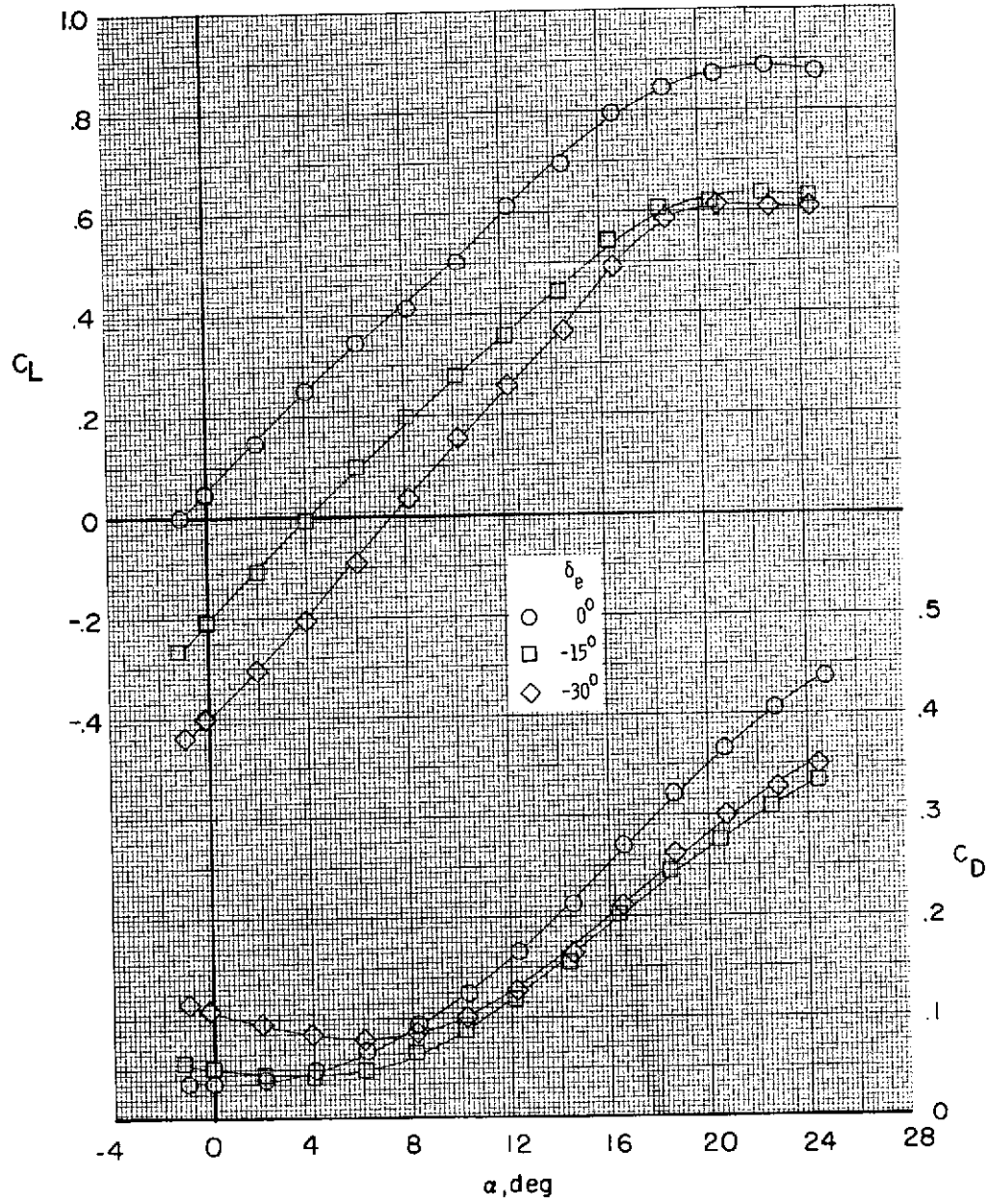

Figure 9.- Effect of elevon deflection on longitudinal aerodynamic characteristics for B9WV. $\delta_{flare} = 30^{o}$; M = 0.8.

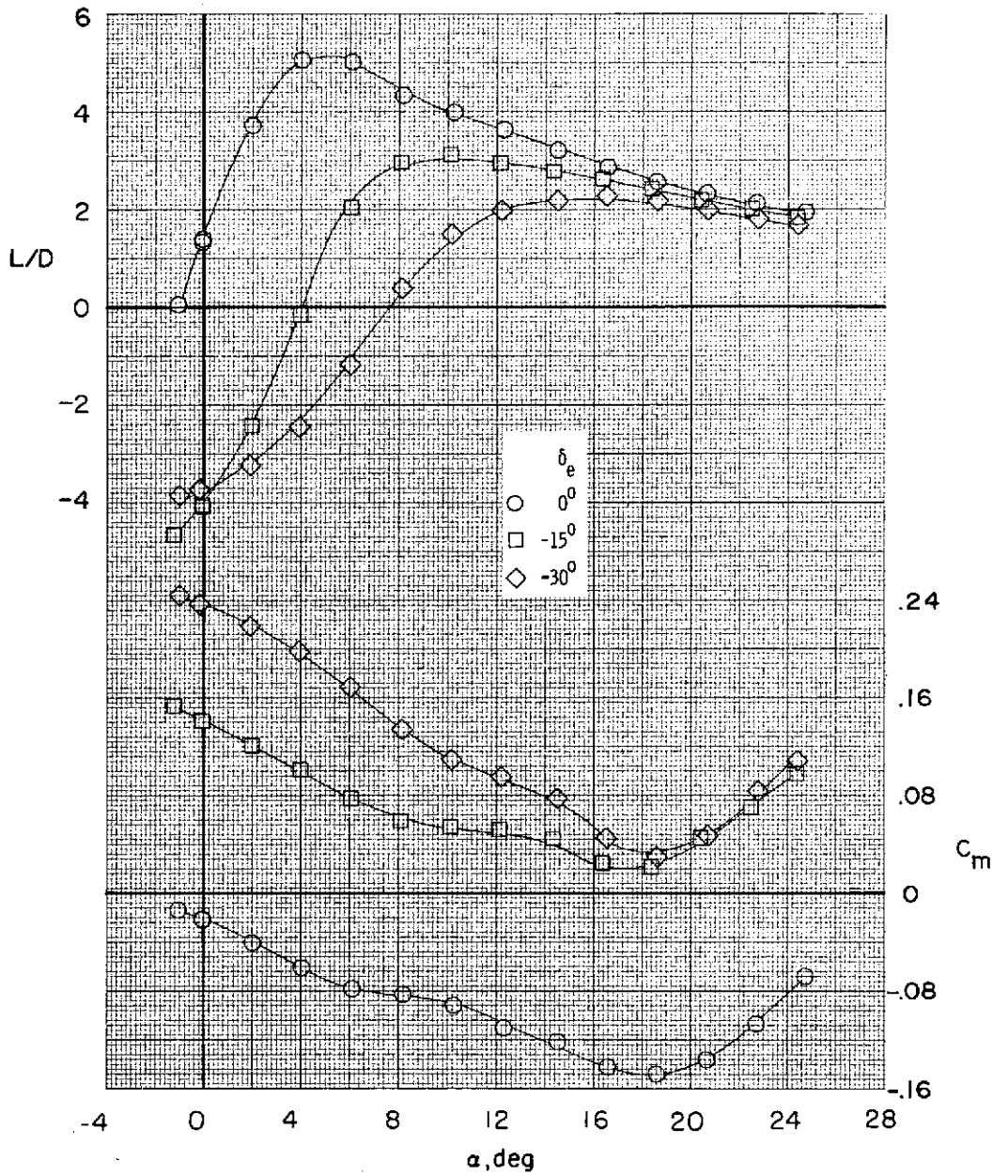

Figure 9.- Continued.

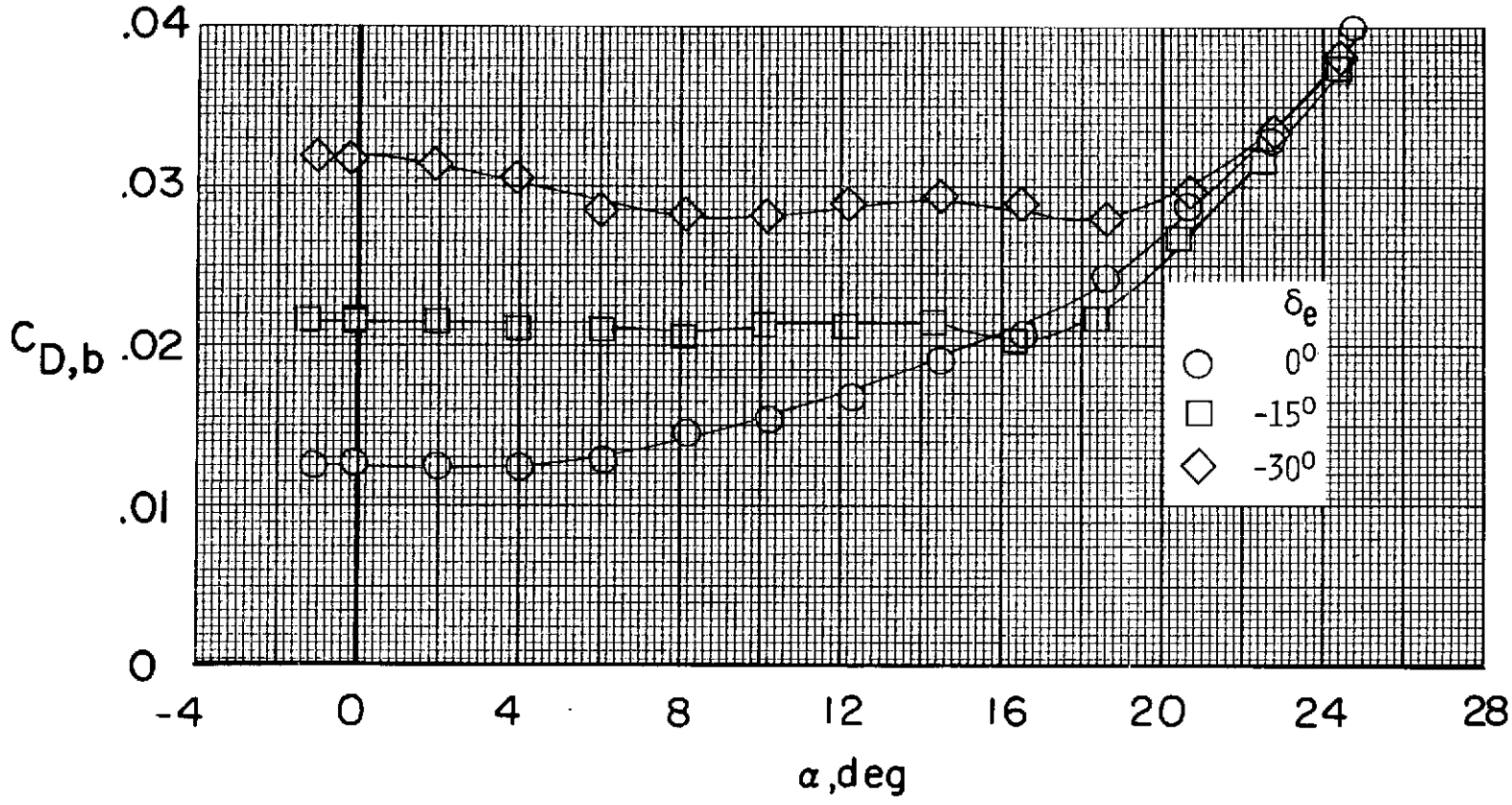

Figure 9.- Concluded.

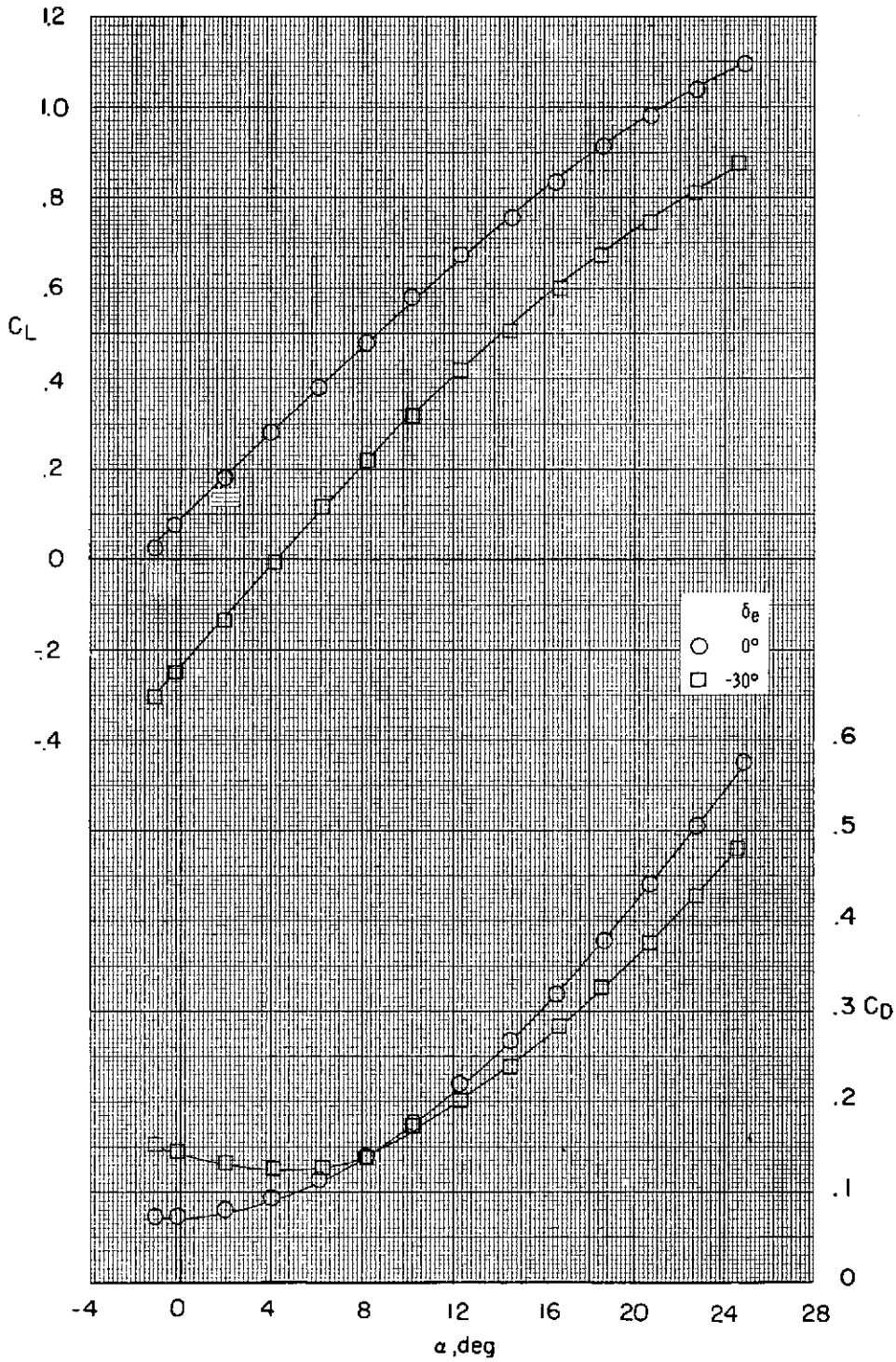

Figure 10.- Effect of elevon deflection on longitudinal aerodynamic characteristics for B5WV. $\delta_{flare} = 30^{o}$; M = 1.2.

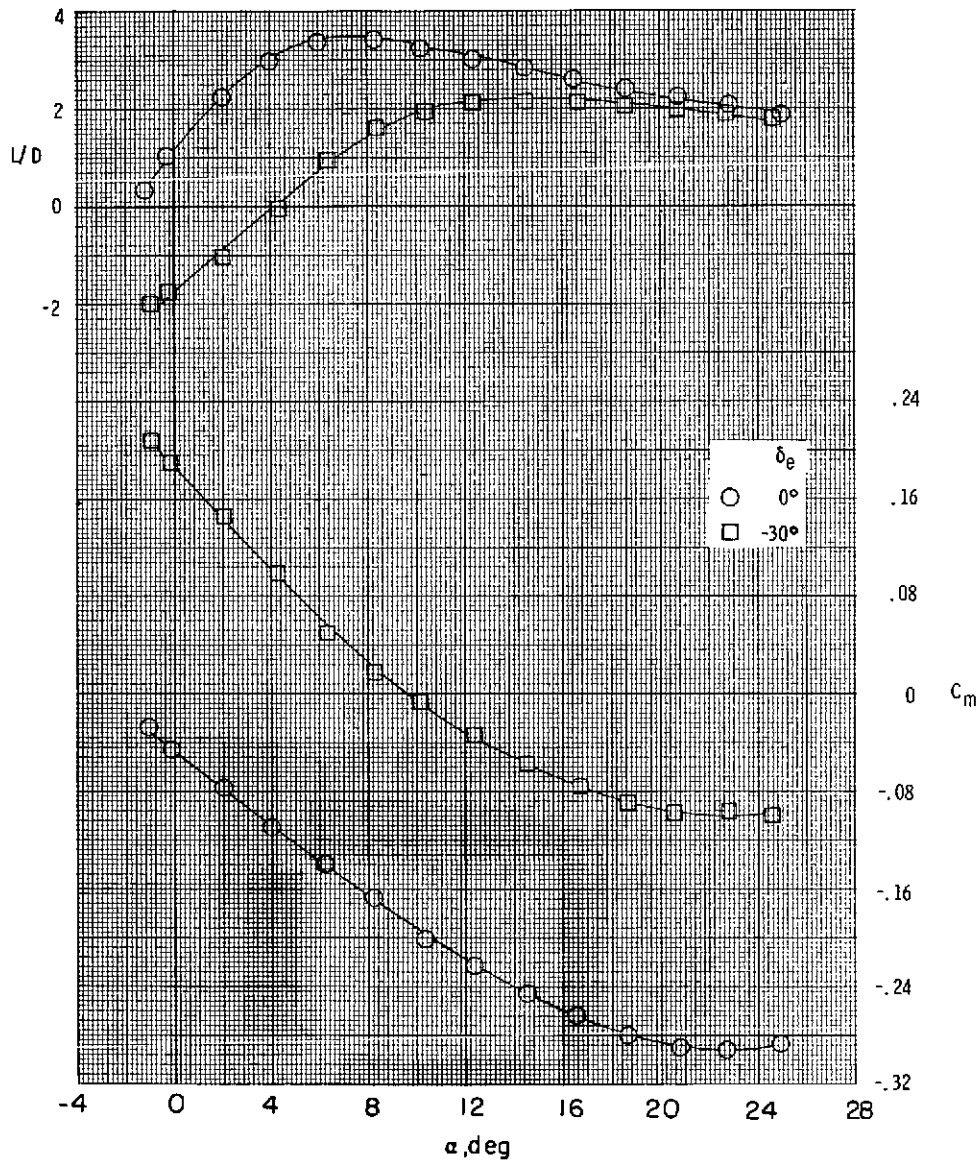

Figure 10.- Continued.

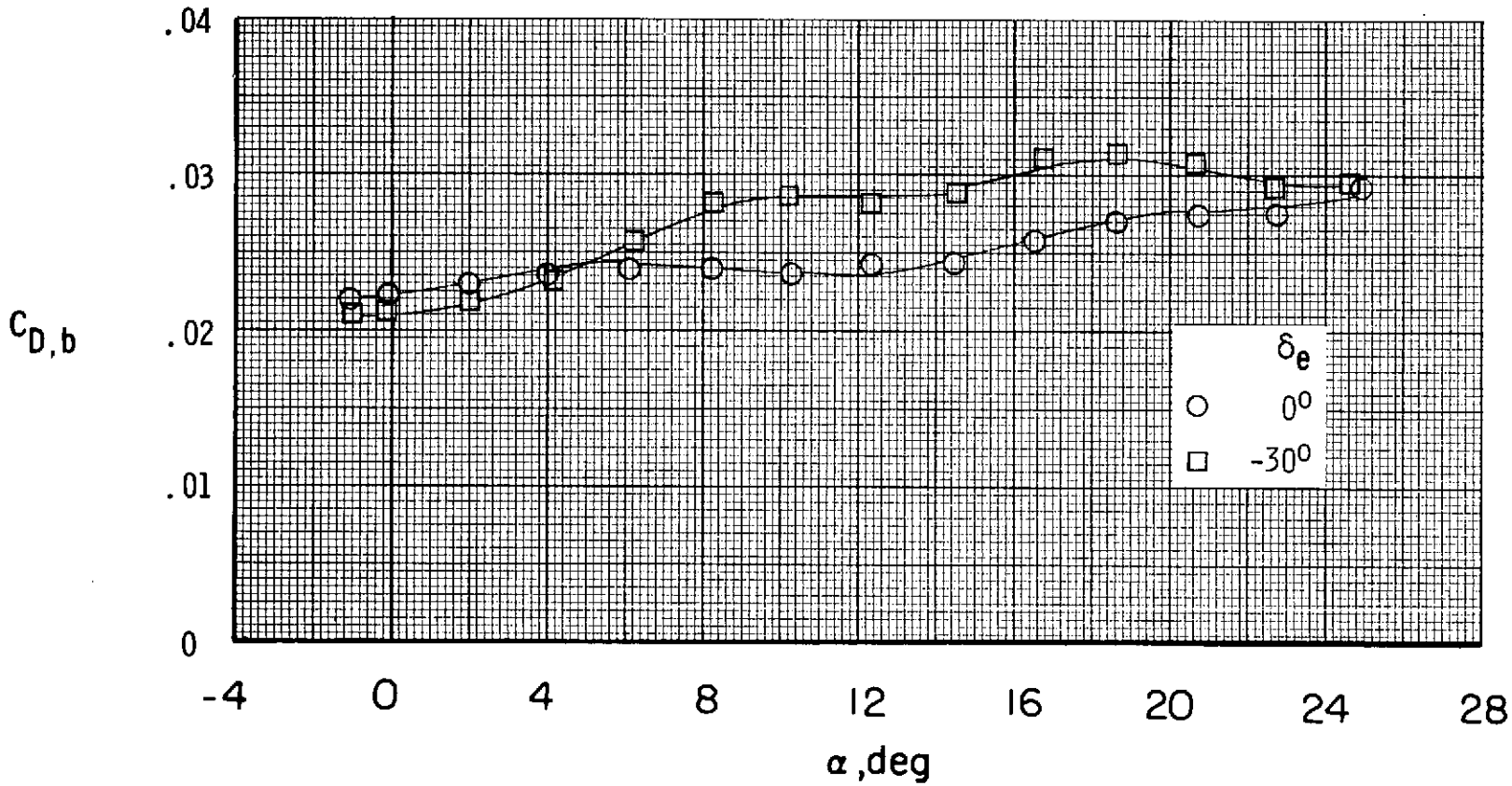

Figure 10.- Concluded.

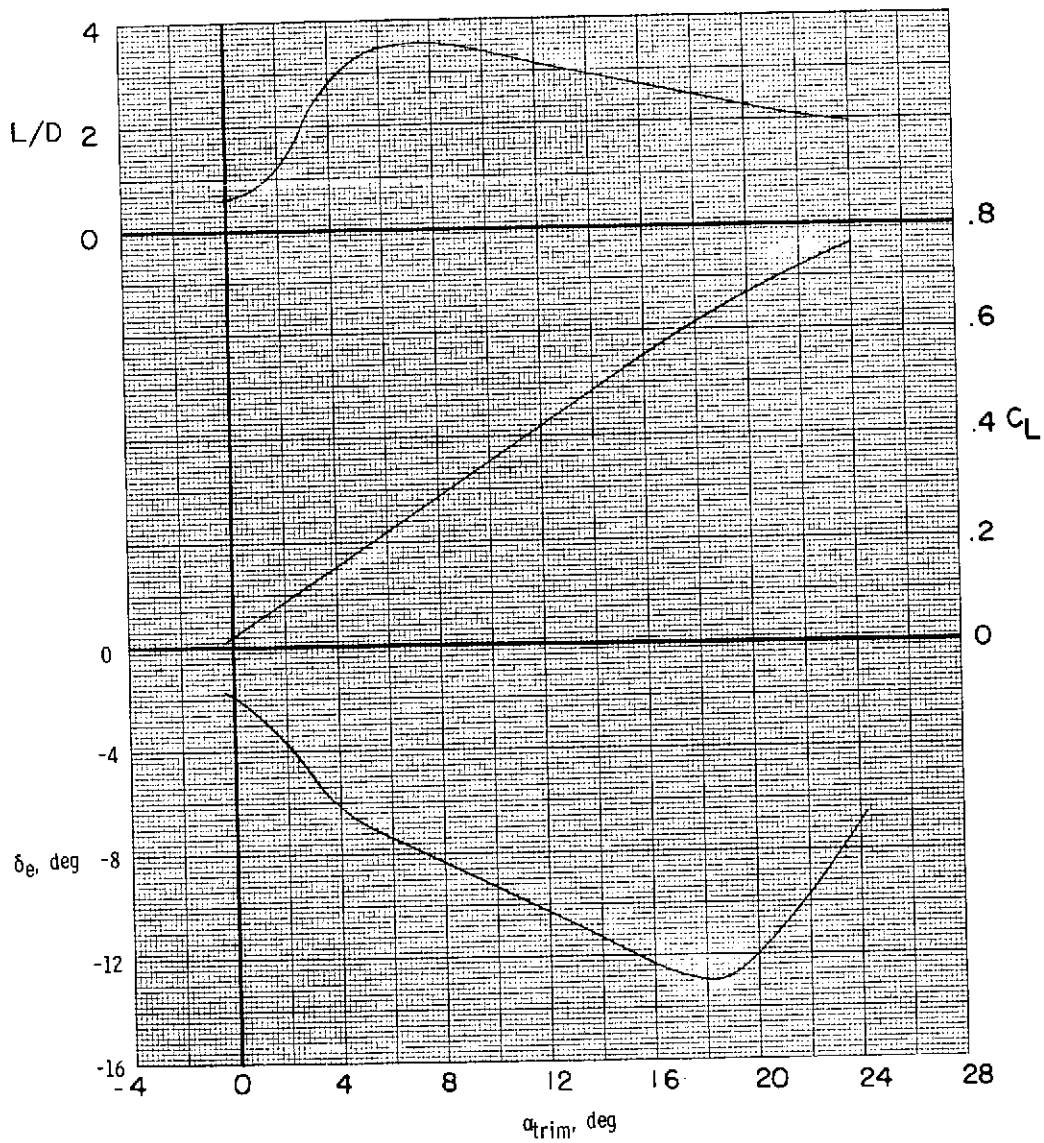

Figure 11.- Trim characteristics of B9WV. $\delta_{flare} = 30^{o}$; M = 0.8.

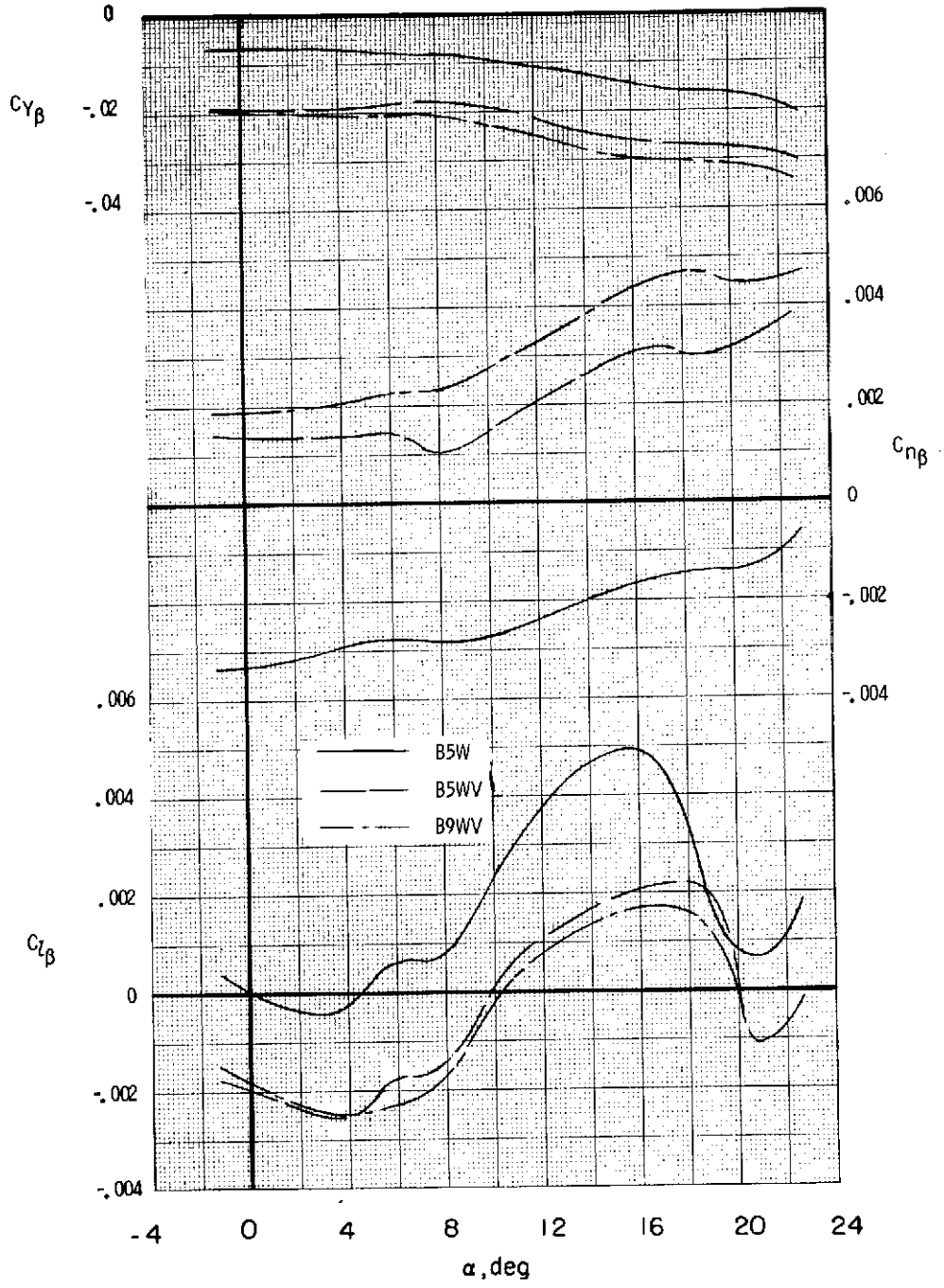

(a) M = 0.8.

Figure 12.- Effect of component buildup on lateral-directional stability characteristics. $\delta_e = 0^o$; $\delta_{flare} = 0^o$.

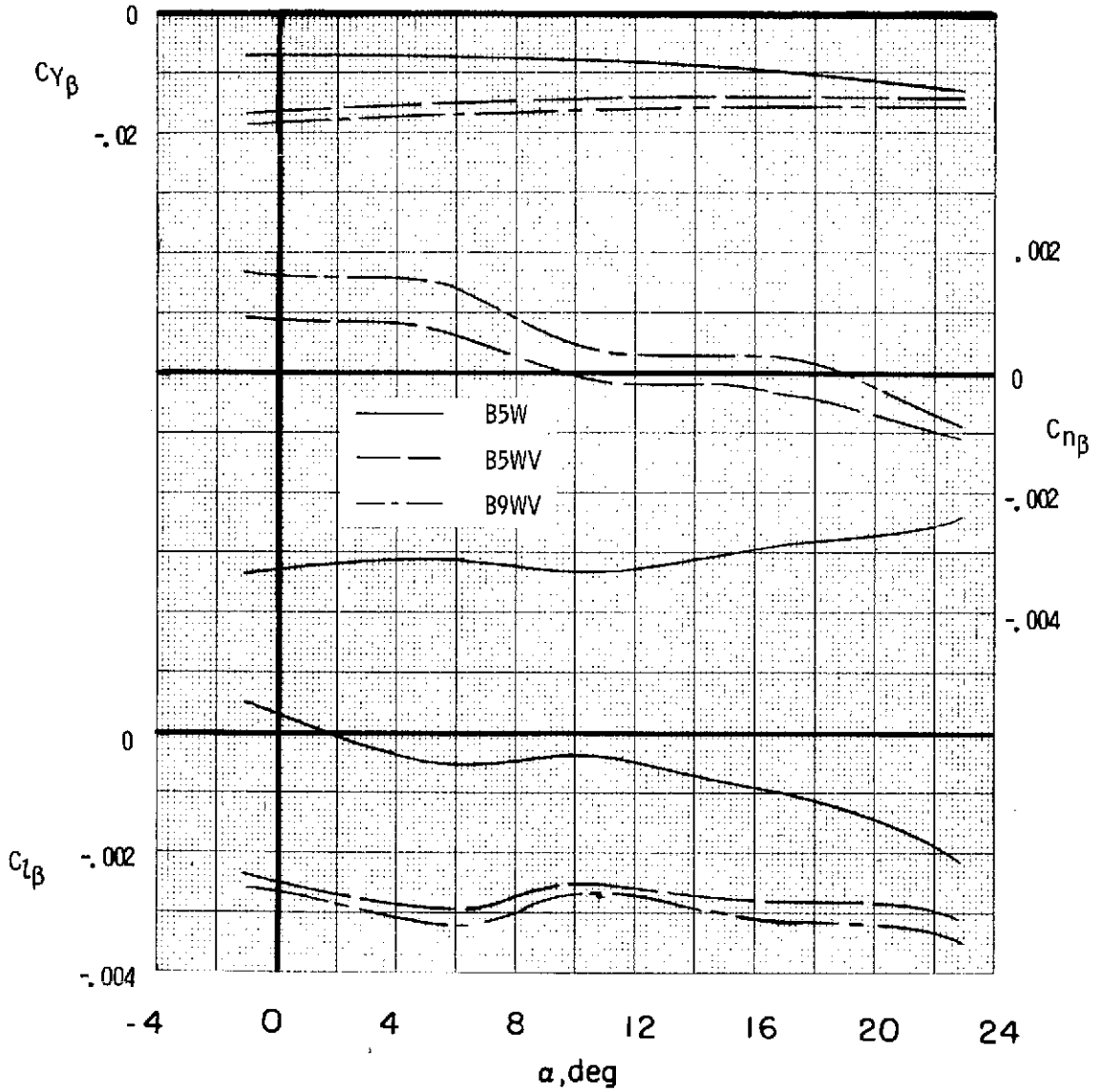

(b) M = 1.2.

Figure 12.- Concluded.

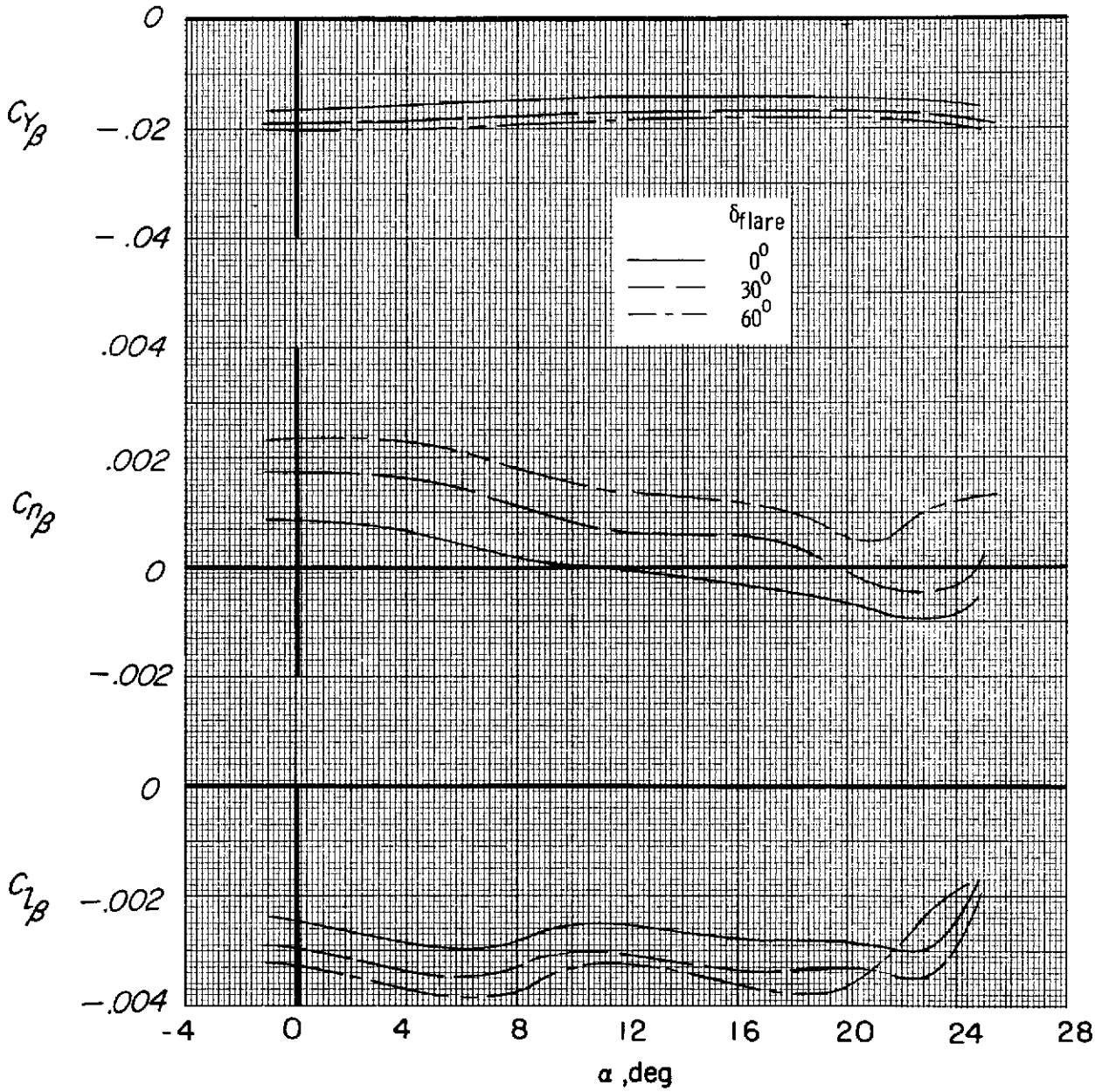

Figure 13.- Effect of rudder flare on lateral-directional stability characteristics for B5WV. M = 1.2; $\delta_e = 0^0$.

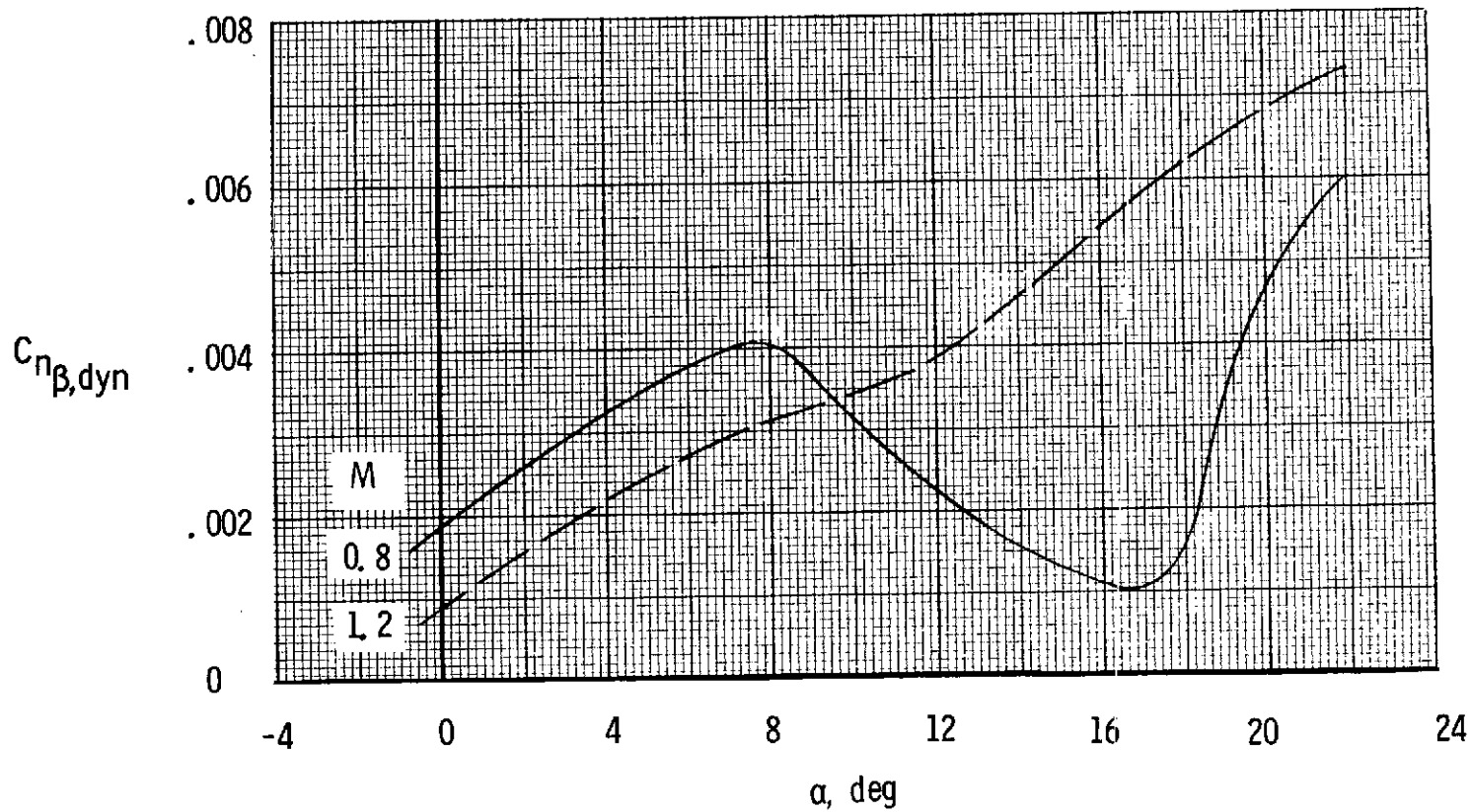

Figure 14.- Calculated values of $C_{n_{\beta,dyn}}$ for B9WV. $\delta_e = 0^o$; $\delta_{flare} = 0^o$; $I_Z/I_X = 6.85$.